Quantitative modelling of mouse limb morphogenesis

Autor: Bernd R. Böhm

TESI DOCTORAL UPF / L'any de la tesi: 2011

DIRECTOR DE LA TESI

Dr. James Sharpe

DEPARTMENT

EMBL - CRG Systems Biology

The research in this PhD thesis was carried out at the Centre de Regulació Genòmica (CRG) in the EMBL Research Programme of Systems Biology and the Department of Experimental and Health Sciences of the Universitat Pompeu Fabra (UPF) located at the Barcelona Biomedical Research Park (PRBB). This research was funded in part by the CRG and by the the Secretariat for Universities and Research of the Ministry of Economy and Knowledge of the Autonomous Government of Catalonia and the European Social Found by means of a fellowship (Ajut FI B) to the author of this thesis.

Acknowledgements

This thesis is dedicated to my parents, Drs. Helga and Heino Böhm, who taught me the value of education and sparked my interest in science. I am deeply indebted to them for their ongoing support and unwavering faith in me even though it wasn't always easy.

First of all I would like to thank my thesis director Dr. James Sharpe who has supported me throughout my thesis with his patience and knowledge and let me return to the lab numerous times. His presentation skills are legendary and I'm thrilled that he was such a good teacher. Invaluable was his guidance and assistance in writing reports and papers, writing this thesis and the included articles would have been impossible without him.

I would like to thank my many colleagues for providing a stimulating and fun environment in which to learn and grow. I am especially grateful to Dr. Jim Swoger for being a good friend, useful discussions in the lab and help in preparation of this document. My special thanks goes to the other members of the lab whose work directly or indirectly contributed to this thesis. Luciano Marcon who was a great help in developing software, Henrik Westerberg for visualization, 3D shape processing and generation of the FEM meshes, Laura Quintana for Sox9 Whole mount in-situ hybridization (WMISH) and image processing as well as OPT scanning, Žiga Jan and Jelena Raspopovic for Sox9 WMISH and Ssq mutant analysis, Gaja Lesnicar-Pucko and James Cotterell for the cell behavior experiments, Sahdia Raja for the BrdU/IddU experiments and the rest of the Sharpe Lab for numerous times helping out with suggestions, help, references etc. and last but not least Michael Rautschka for taking care of my projects while I was away and being a close friend who went with me through thick and thin.
Another big thank you goes to the administration people of the CRG especially to Blanka Wysocka, an absolute gemstone who made so many things possible: in the beginning dealing with gas, water and phone

companies and then to help wherever she could to make a PhD students life easier.

I would like to thank my colleagues and friends that made living in such an exciting city an unforgettable experience. My special thanks goes to Mr. Papi-papa: Filipe Sousa for coping with me for many years being my flatmate and still not being fed up so he and Laura kindly hosted my for the last two month in Barcelona. To Anne Campagna and Sarah Bonnin for many fun and crazy moments. A big kiss to my dear friend Kristin Rossberg for making BCN feel like a home to me, our Döner-dates, being there for me and for showing me the Barcelona-life outside science. Special thanks to Lars Bussmann my brother-in-arms who kept me company in the library whilst writing his own thesis and for his many smart and funny ideas always making me laugh, Anna for a lot of help with organizing my thesis as well as Frank and Rebecca for being my biker-buddies. A big thank you goes to Masha who spiced up my thesis with her English skills.
I would also like to acknowledge my friends from Germany who never let me down even though I've been away for such a long time: Especially Mareike Stubenrauch as well as Christian and Katrin Baun who kept visiting me and for their LaTeX help.

Last but not least, I would like to thank the most important person to me, Jessy. Thank you for your understanding, support and patience in the last two years. Thank you for encouraging and always believing in me.

Für Jörg

Abstract

In this thesis we combine quantitative measurements of mouse limb morphogenesis and computer modelling to test a well established theory about the cellular mechanisms promoting limb elongation. A distally directed gradient of cellular proliferation was believed to be the driving mechanism for limb outgrowth. We find that the empirically measured spatial proliferation pattern fails to promote normal development - a reverse engineering algorithm was applied and revealed a proliferation pattern that could indeed carry out normal development. The differences between those patterns is dramatic and suggests that isotopic cellular proliferation alone has very little impact on limb morphogenesis and other - non isotropic - mechanisms need to be involved.

Resumen

En esta tesis tratamos de testar una bien establecida teoría sobre los mecanismos celulares que promueven de la elongación de las extremidades. Para eso combinamos mediciones cuantitativas del proceso morfogenético de la extremidad del ratón con modelos computacionales. Se creía que la fuerza conductora del crecimiento de las extremidades era un gradiente en sentido distal del incremento de la proliferación celular. Descubrimos que el patrón de proliferación celular basado en medidas empíricas no conseguía promover un desarrollo normal, mientras que un algoritmo de ingeniería inversa aplicado al proceso reveló un patrón que si podría. La diferencia entre estos dos patrones es inmensa y sugiere que la proliferación celular isotropica por si sola tiene muy poco impacto sobre la morfogénesis de las extremidades, indicando así la necesidad de que otros procesos no isotrópicos se hallen involucrados.

Preface

The vertebrate limb bud has been studied for decades as a model system for spatial pattern formation and cell specification, yet the cellular basis of limb elongation remains unclear. The most popular hypothesis is that a gradient of proliferation exists along proximal-distal axis of the limb. High proliferation rates at the distal tip and lower rates towards the body are believed to be the driving force behind outgrowth. Within the relatively short period of 36h the limb rapidly elongates from initially being a homogeneous ball of mesenchymal tissue into a collection of spatially arranged, differentiated cells. The main objective of this thesis was to test this hypothesis of "growth based morphogenesis" by combining quantitative empirical data sets with computer modelling, to assess the influence of cell proliferation rates on limb bud outgrowth. We also present a new tool which is capable to quantify time during limb development - a morphometric limb staging system. We describe a method to classify the age and development of a limb bud [Boehm et al., 2011]. We have created a staging system for 2D images of mouse hind-limb. For our staging system we captured the shape information of approximately 650 limb buds of carefully controlled gestational ages and extracted the standard trajectory of limb development from mE10:09 to mE12:21 in one hour apart time steps. Further we developed a web based user interface that allows registered users with internet access to use this system to stage their own data on a standard Pc.
In a different study [Boehm et al., 2010], we generated two empirical data sets for the mouse hind limb - a numerical description of shape change and a quantitative 3D map of cell cycle times. The shapes were quantified by Optical Projection Tomography (OPT) a 3D microscopy technique and the temporal difference between the shapes was quantified by the previously developed morphometric staging tool. The data was combined with a new 4D finite element model of tissue growth. By running a simulation of this model we discovered, that empirically measured spatially distribution of proliferation rates plays no significant role in distal outgrowth. This was subsequently validated by developing a reverse en-

gineering technique that revealed a hypothetical proliferation patter that would promote the expected outgrowth. As the empirical and the hypothetical proliferation pattern show a tenfold difference we suggest that not isotopic, but directional cell activities are likely to be the driving force behind limb bud outgrowth. This theoretical prediction prompted us to search for evidence of directional cell orientations in the limb bud mesenchyme, and we thus discovered an extended cell shape of mesenchymal cells, showing long dynamic filopodia, a distally oriented bias in Golgi position, and also a bias in the orientation of cell division towards the ectoderm. We therefore provide both theoretical and empirical evidence that limb bud elongation is achieved by directional cell activities, rather than a Proximo-distal (PD) gradient of proliferation rates.

Contents

Chapter 1

INTRODUCTION

The goal of this thesis is to improve our understanding about the cellular processes of limb morphogenesis. To achieve this we employ a combination of inter-disciplinary techniques to accurately measure its development and the cellular processes involved. Computer simulations help answering the question, how empirically measured cell proliferation patterns influence the shape of the developing limb and parameter optimization helps to find a cell proliferation pattern that resembles empirically measured limb morphogenesis. The approaches of "quantification" and "simulation" are two of the basic principles of *Systems Biology*. A brief introduction to the limb as a model system, the concepts and philosophy of Systems Biology, the quantification of limb development, and modelling in science is given here.

1.1 Limb development

In this thesis the limb development of *Mus Musculus*, a popular model system for pattern formation and cell specification, was studied. In particular we were interested in the cellular processes which are not well understood.

1.1.1 The mouse as a model system

Model organisms are species that have been widely studied, usually because they were easy to maintain and breed in a laboratory setting and had particular experimental advantages. The most popular model organisms include the bacterium *Escherichia coli* and its bacteriophage viruses, bakers' yeast *Saccharomyces cerevisiae*, the nematode worm *Caenorhabditis elegans*, the fruit fly *Drosophila melanogaster*, the mustard plant *Arabidopsis thaliana*, the zebrafish *Danio rerio*, and the frog *Xenopus laevis* as well as the mouse *Mus musculus*. Each of those species have their advantages e.g. yeast for studying the cell cycle, cell polarity and RNAi, and E.coli is the popular model for studying metabolism and general aspects of molecular genetics. The *Mus Musculus* is an ideal model organisms for biomedical research: Mice have been bred for centuries, mostly to create "fancy mice" with an interesting color or pattern and their mating and maintaining is well studied. They are easy to maintain and to breed and a diverse population of animals is available. Mice are small and reproduce quickly, some strains can produce as much as one litter per month with approximately 10-15 embryos. In 1911 Clarence Cook Little achieved breeding "pure" i.e. inbred strains and showed that these were genetically almost identical. The advantage of fixation of the genetic background is the reproducibility of experiments in different laboratories and through time. Mice and humans share a high degree of homology in their genome (Figure 1.1), so many human genes of interest can be studied in the homologue in mice. Another advantage over other model organisms like the chick is the highly advanced gene transfer technology available to create transgenic specimens. Researchers can revert to a big stock of mice carrying almost any foreign gene of interest. Various mouse strains have been especially designed for research: Some are specially bred for behavioral studies (NMRI) whereas others are models for studying diabetes (NOD). C57BL/6 black six from the Jackson Laboratory are the most widely used (inbred) lab mouse strain, due to the availability of congenic strains, easy breeding and robustness.

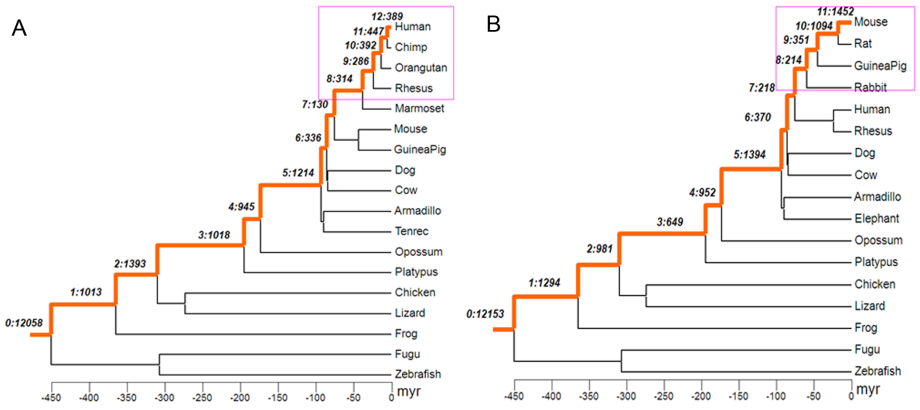

Figure 1.1: **Phylogenetic tree of vertebrates.**
Branches leading to human and to mouse are marked as orange lines. (A) and (B) show the assignments of new genes to branches on the phylogeny of human an mouse, respectively. The young genes, those primate- and rodent-specific, are marked with pink boxes. The notation with two numbers separated by ":" indicates the branch assignment and the number of genes occurring in the given branch. For example, in the human lineage represented in (A), in branch 12, 389 genes originated after the split of humans and chimps. Due to different annotations in mouse and human, the number of genes gained may differ, adapted from [Zhang et al., 2010].

1.1.2 The limb as a model system

The limb bud is one of the classical model systems in developmental biology. Even though the adult limb bud varies in size and shape among different species and even between fore and hind limb, the underlying molecular cues are highly conserved. As an external organ it is easily accessible for various classical manipulation techniques. The development is relatively independent from the body of the embryo, which limits the complexity of body-limb genetic interactions. Studying limb development has contributed to some of the key concepts in the developmental field like the progress zone model [Saunders, 2002, Saunders, 1972], positional information and the French Flag model [Wolpert, 1969, Wolpert, 1968]. The latter model is based on the idea that cells acquire positional identities defined by boundaries on a morphogen gradient secreted by a signaling center. Initially most limb experiments were performed in chick due to easy accessibility, but gradually the mouse became more and more relevant. These two species are currently the two main model organisms but the bat wing, the axolotl limb, the three-toed jerboa [Cooper et al., 2010] and also the wallaby limb [Pask et al., 2002] were recently used as models to study aspects of limb development. The limb has been worked on for decades and great progress has been made in understanding the molecular processes involved in patterning and cell specification, although limb development is not fully understood yet. In addition to being an ideal model system for the study of many genetic and molecular processes it is also a good evolutionary model as the limb is a homologous structure found in all tetrapods (Figure 1.2). The developed limb has one single proximal bone (humerus), two distal bones (radius and ulna), a series of carpals followed by five series of metacarpals and phalanges (digits). This fundamental structure is conserved among tetrapod species, although it has been adapted in the course of evolution to serve specific purposes.

The medical implications of limb malformations are diverse: Our hands and feet are of high relevance to our interactions with the world. Malformations can significantly decrease the life quality of an individual but are also often linked to severe clinical conditions too. It has been shown,

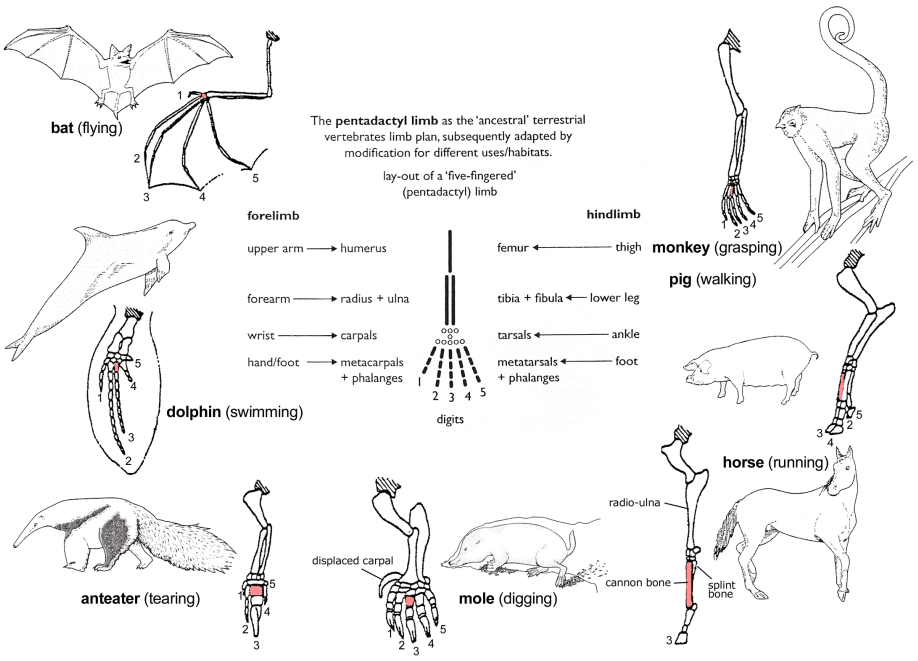

Figure 1.2: **The limb as a homologous concept.**
Illustrated are the adaptive modifications of the forelimb, conserved among mammal species. They all share the basic pentadactyl pattern but are modified for different usages. Obtained from wikipedia.com - Evidence of evolution.

that upper limb malformations are often associated with congenital heart diseases [Lin and Perloff, 1985]. A few more examples are: The Pfeiffer syndrome which is characterized by the premature fusion of bones and affect the growth of the scull and the shape of the face as well as hand and foot digital anomalies due to mutations in the Fibroblast growth factors [Chan and Thorogood, 1999]. The Rubinstein-Taybi syndrome which is characterized by moderate to severe learning difficulties, distinctive facial features, and broad thumbs and first toes [Petrif et al., 1995]. Hirschsprung disease (HSCR), or congenital intestinal aganglionosis is a common hereditary disorder (1/5000 births) affecting the function of colon often resulting in obstructions. Even though mostly not showing a limb phenotype, mutant studies in mice indicate that Sonic Hedgehog (Shh) and Indian Hedgehog (Ihh), both important during limb development, have individual and overlapping functions in the development of the gut as well [Ramalho-Santos et al., 2000]. Ihh –/– mice develop HSCR, suggesting that HH signaling may play a role in the pathogenesis of the disease.

1.1.3 Structure of the limb bud

In the mouse and chick, the limb bud starts as a small bulge from the lateral flank of the embryo. It possesses a very simple structure, composed of a central mass of mesenchymal cells covered by a single-cell ectodermal epithelium. Very early in development the ectoderm develops a thickened ridge (the Apical ectodermal ridge (AER)) which runs along the Antero-posterior (AP) axis and marks the anatomical boundary between dorsal and ventral ectoderm (Figure 1.4). Over the next 36 hours the limb bud elongates away from the body flank while changing shape from a ball like to a flat paddle shape which shows first signs of digits also visible in the expression of Sox9 (see Figure 4 [Boehm et al., 2011]). This patterning process is well studied since the limb first came into the focus of researchers half a century ago.

1.1.4 Patterning of the limb along 3 axes

Patterning is the process of cell specification to form organized structures like bones, muscles and tendons. During limb development this happens along the three main axis: AP, Dorso-ventral (DV) and Proximo-distal (PD). Two main signaling centers are involved in the patterning process: The Zone of polarizing activity (ZPA) and the AER. Experiments early in the 1960s [Gasseling and Saunders Jr, 1961, Bell et al., 1959] uncovered the essential role of the AER for normal outgrowth. Surgical removal of the AER from the bud of a chick embryo (*in-ovo*) resulted in a truncation of the wing, which lacked the distal part of the skeleton. This showed that the AER is a major signaling center for limb bud development and also inspired the progress zone model [Saunders, 2002, Saunders, 1972]. Similar "cut-and-paste" experiments from other labs were able to identify two further centers: the ZPA [Rubin and Saunders, 1972], a posterior region of mesenchyme required for patterning along the AP axis, and the dorsal ectoderm, which controls differences along the DV axis.

1.1.5 The ZPA

The ZPA (Figure 1.3) is a small posterior region of mesenchymal cells required to promote asymmetries along the AP axis (e.g. the difference between the fingers and thumb). It was first described in 1968 [Saunders and Gasseling, 1968] and can induce mirror-image duplications of the digits when grafted to the anterior of a different limb. The ZPA was believed to produce a morphogen which forms a gradient across the early limb bud. According to this model, cell fate at different distances from the ZPA is determined by the local concentration of the morphogen, with specific thresholds of the morphogen inducing successive structures [Wolpert, 1969]. In 1981 Tickle showed [Tickle, 1981] that the extent of digit duplication is proportional to the number of implanted ZPA cells, which supports the idea of concentration-dependant pattern formation. In 1993 [Riddle et al., 1993] showed that Sonic Hedgehog (Shh) which is expressed in the ZPA from E9.5-E9.75, plays a key role in the AP patterning of the limb.

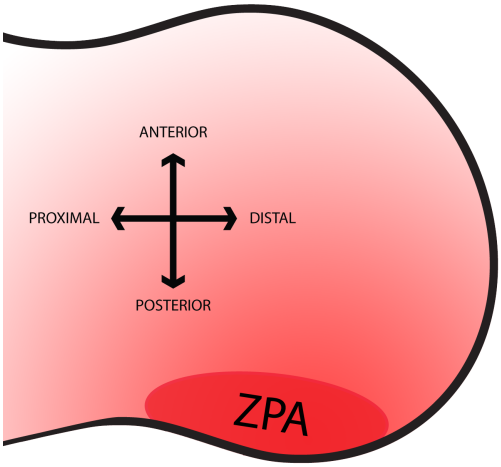

Figure 1.3: **The ZPA**
The ZPA is a main signalling center in the limb bud controlling AP patterning, as one of the most important signals it secretes Shh - an important regulator for bone specification.

Recent studies have discovered a positive feedback loop between the AER and the ZPA: It was shown that beads soaked in Fibroblast growth factor (Fgf) rescue Shh expression and outgrowth after AER removal, and that *vice versa* ectopic Shh beads induce AER-Fgf expression [Benazet et al., 2009, Tickle, 2005, Niswander, 2002]. As Fgf8 expression appears before Shh in the limb, Shh signalling is not required for the initiation of Fgf8 expression but rather *vice versa* [Lewandoski et al., 2000, Moon and Capecchi, 2000]. So experiments in mouse and chick have shown that in the absence of AER-Fgfs, no Shh expression could be found [Ros et al., 1996] or reduced expression in Fgf8 mutants [Sun et al., 2002].

1.1.6 The AER

The apical ectodermal ridge (Figure 1.4) is a thickened ridge at the distal tip if the limb [Saunders, 1948]. It is one of the main signalling centers in the limb bud and plays a key role in limb initiation. The AER emerges from the ectodermal layer covering the Lateral plate mesoderm (LPM), where Wnt3, β-catenin and Fgf form a regulatory loop involved in AER establishment and maintenance as well as in the control of limb initiation [Barrow et al., 2003]. Fgf10 signals from the LPM are received by the ectoderm, where a feedback loop with Fgf8 initiates limb formation. The fore- and hindlimb buds of the mouse embryo first appear as bumps on the flank adjacent to somites 7-13 and 27-31 during the 10th and early 11th days of gestation [Ohuchi et al., 1997]. In the chick the AER forms soon after the limb bud bulges out, whereas in the mouse the AER does

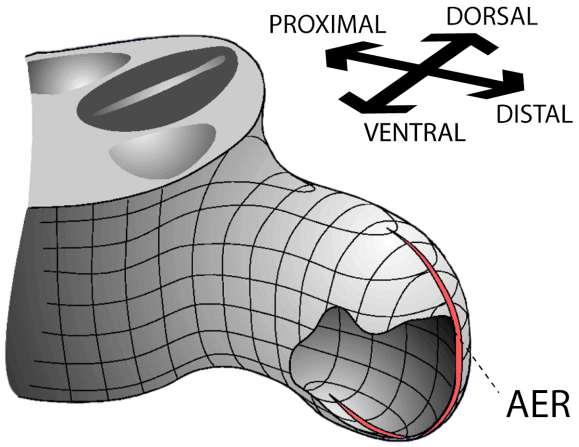

Figure 1.4: **The AER**
The AER is a thickened ridge at the most distal part of the limb. It runs anterior posterior and marks the boundary between dorsal and ventral part of the limb. It is believed to be a main signalling center important for limb outgrowth.

not form until limb outgrowth has progressed [Wanek et al., 1989]. The signals from the AER are crucial for normal limb outgrowth: A classical experiment [Saunders, 1948] showed that removal of the AER resulted in truncation of the limb bud and the loss of distal structures. Removal of the AER even in earlier stages resulted in increased limb truncation beginning with the most distal elements. Fgf2 soaked beads applied after AER removal can rescue relatively normal limb development in chick. [Fallon et al., 1994] Also Fgf4 was shown to maintain normal limb outgrowth in the absence of the AER [Niswander and Martin, 1993a]. Beads soaked in Fgf1, 2 or 4 were shown to be capable of inducing (additional) ectopic limb buds when placed at the presumptive flank of the chick embryo. [Cohn et al., 1995] The roles of the AER-Fgfs were studied in several papers [Lewandoski et al., 2000, Moon and Capecchi, 2000, Boulet et al., 2004, Mariani et al., 2008]. Mariani *et al.* genetically deactivated numerous members of the Fgf family (4, 9, 17) and showed that only silencing Fgf8 caused an AER related phenotype. Limb outgrowth was delayed, the AER reduced in size and the limb lacked some skeletal elements. Although Fgf4 inactive mice show nearly normal phenotypes, Fgf4 can be upregulated in Fgf8 deficient mice and partly compensate for the loss. Fgf4/8 compound mutants show a complete agenesis of skeletal elements during early inactivation or a notable smaller limb bud during later deactivation.

1.1.7 Models for molecular patterning

The progress zone model has sometimes been confused with the mechanism for limb outgrowth, as the AER also signals Fgfs stimulating cell proliferation. It suggests that signals from the AER maintain an underlying region of mesenchymal cells (the progress zone) in an undifferentiated state. Summerbell, Lewis and Wolpert [Summerbell et al., 1973] first introduced the idea of the progress zone to explain the patterning of the limb bud along the proximal-distal axis. The model states that progressive proximal-distal specification depends on the time cell remain

in a region just under the AER in which proximal fate is specified first, followed by more distal specification. As the limb grows, cells are forced out of the progress zone, at which point the positional value that they acquired within the progress zone is fixed. Thus, cells that leave the progress zone first produce more proximal structures and as development progresses, longer remaining cells will be specified to form more distal structures.

1.1.8 Models for mechanical outgrowth

The most prominent hypothesis - the "proliferation gradient model" was first described in [Ede and Law, 1969], and only few papers since have analyzed the cellular processes involved in limb elongation. Their idea was that a diffusible signal from the AER acts as a mitogen which stimulates the mesenchyme immediately underlying it to proliferate. This proliferating zone promotes directly distal outgrowth. Though they already formulated doubts about the sufficiency of their hypothesis to explain limb morphogenesis by a pioneering computer model, it remained the most popular idea. It was supported by some classical studies [Reiter and Solursh, 1982, Summerbell and Wolpert, 1972, Hornbruch and Wolpert, 1970] and some more recent papers, reporting a PD-graded distribution of proliferation rates in mouse and chick limb buds [Dudley et al., 2002, Fernandez-Teran et al., 2006]. Further the diffusible molecules - Fgf4 and Fgf8 - were discovered to be expressed in the AER [Niswander and Martin, 1992, Niswander and Martin, 1993b], and show mitotic influence in various organ systems [Xu et al., 2000, Prykhozhij and Neumann, 2008] therefore being favorable candidates for a hypothetical mitogen. A computer simulation [Dillon and Othmer, 1999] studied the cellular processes during limb development by a 2D finite element model. They incorporated the idea of a distal, diffusible mitogen into their immerse boundary Finite element modelling (FEM). They didn't challenge the hypothesis directly but also found no contradiction. Recently computer simula-

tions were published that directly tested the proliferation gradient model: Poplawski *et.al.* implemented the proliferation gradient model in to a Cellular Potts framework to show its sufficiency to explain distal limb outgrowth [Poplawski et al., 2007]; Morithita and Iwasa chose a cell-based Spring-lattice model also in 2D and demonstrated similar results [Morishita and Iwasa, 2008], they named the theory "*growth-based morphogesis*" which is from now on, referred to.
Alternative hypothesis have been formulated: Lewis Wolpert suggested that mechanical forces from the ectoderm may have a shaping effect on the growing limb bud [Hornbruch and Wolpert, 1970]. Yet it has been demonstrated that limb development is rather normal in the absence of dorsal ectoderm [Saunders, 1948, Martin and Lewis, 1986, Boehm et al., 2010] and (Figure 3.14) therefore the mechanical shaping effect of the ectoderm seems at most marginal. Wolpert also formulated another theory in the same paper that oriented cell division may be involved in limb outgrowth. The principal is known from other morphogenic processes such as vertebrate gastrulation [Gong et al., 2004] and *drosophila* wing disk development [Baena-López et al., 2005]. Until recently there was no evidence for this, although in [Boehm et al., 2010] we have shown the first indicators that indeed oriented cell behaviors can be observed in chick and mouse. Further studies in our lab and recent publications [Wyngaarden et al., 2010, Gros et al., 2010, Wang et al., 2011] support our research.

1.1.9 Summary

Recent studies have reported, that *growth-based morphogenesis* can be the driving mechanism behind limb morphogenesis. A gradient in cellular proliferation was repeatedly found, candidates to account for the role as a mitogen discovered and computer simulations incorporating this, from the AER secreted signal showed plausible limb elongation. Yet, the models lacked quantitative data and the main objective of this thesis was the systematic study of the sufficiency of this hypothesis as an explanation for limb outgrowth by applying a Systems Biology approach.

1.2 Systems Biology

A number of ideas and concepts of Systems Biology are introduced in this chapter. Initially they mostly played a role in the study of genetic interaction. However we studied the use of applying them to a developmental question - the role of cellular proliferation in limb development.

1.2.1 History of Systems Biology

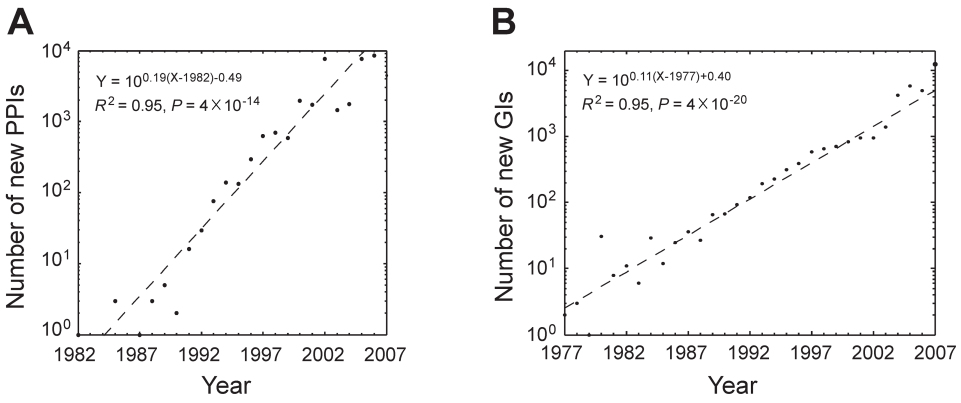

Figure 1.5: **Numbers of new interactions discovered each year in the yeast.**
(A) protein-protein interaction (PPI) network and (B) genetic interaction (GI) network. Obtained from [He et al., 2009].

Scientific knowledge is increasing exponentially as shown recently by [He et al., 2009] by the examples of protein interactions and genetic interactions in baker's yeast (Figure 1.5), but:
The more we know about genes, the less we understand [Zimmer, 2008].
This means, the deeper our understanding about biological systems like baker's yeast goes, the more we need to acknowledge the complexity of the underlying genetic processes and our inability to fully understand

them. The dynamical, non-linear interactions can only be fully understood by considering them as one interconnected system. Individual interactions, isolated from the rest of the involved genes and proteins, contribute little to a general understanding how a living organism works. It is widely recognized that our ability to treat complex diseases like Alzheimer disease, Diabetes mellitus, nicotine and alcohol addiction, Parkinson disease and several cancers, will depend on a systems-level understanding of such complex genetic processes.

Systems Biology is a new field of science which tries to achieve such a general understanding by combining several different scientific approaches, such as computer science, physics, math and engineering. Systems Biology approaches are often applied to study genetic networks however the concepts are also applicable to other fields of biology such as development. The general concepts are introduced here in the classical genetic context.

Systems Biology has evolved from the initial idea described in [Wiener, 1948], into a scientific buzzword [Bonetta, 2002], and then into a whole paradigm change in biomedical research. A Google Scholar search for Systems Biology related publications in the last 15 years shows a stable increase (Figure 1.6) in the number of publications, indicating that this "fashion" has been widely accepted from the scientific community.

For decades researchers followed the reductionist approach of identifying single components of complex biological systems such as individual genes and proteins. This process was slow but an impressive amount of knowledge has been generated. With the recently developed -omics methods it has been possible to rapidly generate enormous amounts of data even on a the very low level of signalling pathways; however it has become more and more evident that this on its own does not automatically lead to comprehensive understanding of the studied system. How do the individual parts interact and how does the system respond to perturbations? Classical molecular biology lacked convincing concepts and methods to find answers to these questions [Sauer et al., 2007].

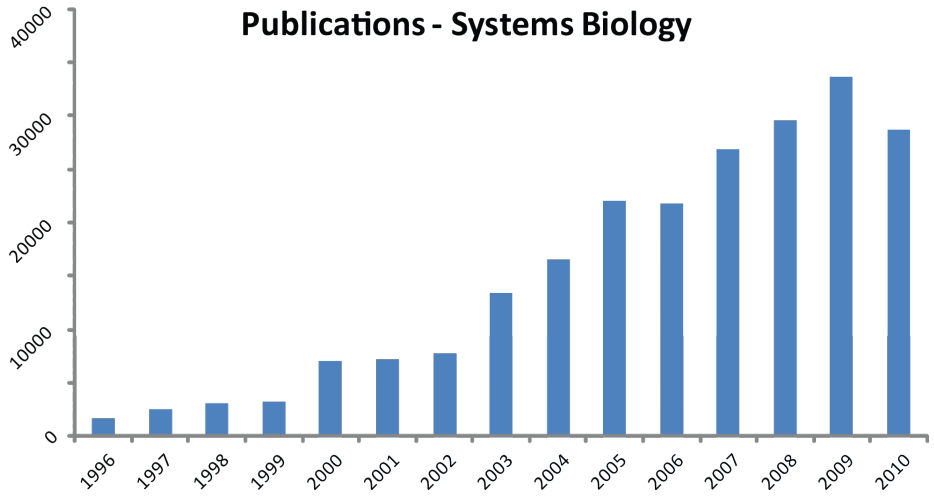

Figure 1.6: **The increase in Systems Biology publications.**
Since 1996 the number of scientific publications using the "buzzword" systems biology, shows a stable increase without losing the "buzz".

Identifying all the genes and proteins in an organism is like listing all the parts of an airplane. While such a list provides a catalog of the individual components, by itself it is not sufficient to understand the complexity underlying the engineered object. We need to know how these parts are assembled to form the structure of the airplane. This is analogous to drawing an exhaustive diagram of gene-regulatory networks and their biochemical interactions [Kitano, 2002].

Classical biology approaches fail to deliver comprehensive data required for inferring regulatory mechanisms. E.g. mutant knock out studies show a lack of (1) quantification (2) consistency (3) uniqueness and (4) completeness [Jaeger et al., 2004] which are essential factors for building a reliable model.
The lack of quantitative data makes it difficult if not impossible to test a hypothesis. The problem is highlighted in the example of the

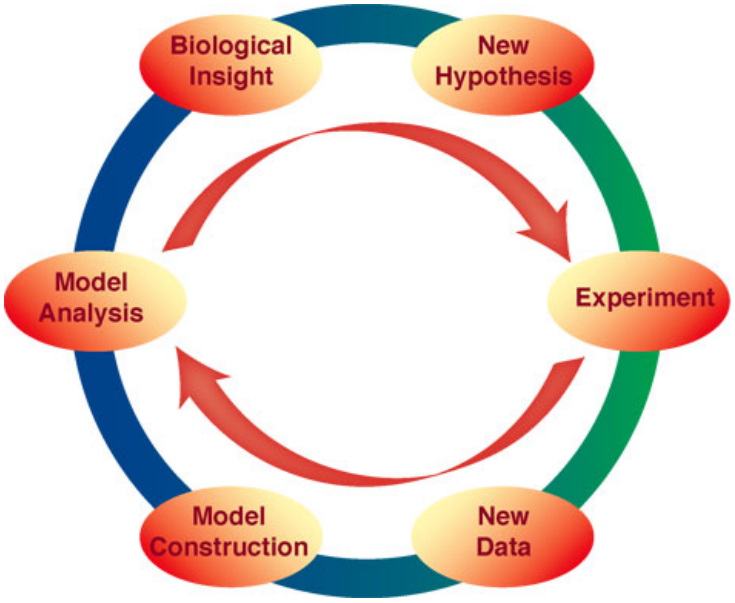

Figure 1.7: **The "wheel" of systems Biology.**
The process involves repeatedly and iteratively improving a hypothesis, experiments, models to get new biological insights (obtained from http://www.doc.ic.ac.uk/bioinformatics/CISB/).

temperature of a closed vessel with an ideal gas. If the hypothesis was that by increasing the pressure by 10%, the temperature will rise by 10% , then the qualitative test to the hypothesis would be: The temperature does or doesn't increase and therefore the test has a 50% chance of being passed by coincidence. The quantitative test gives a far more precise answer with a much reduced chance of being right by coincidence [Boogerd, 2007]. Consistency of a proposed regulatory mechanism can only be established by monitoring all regulatory inputs to a specific gene [Reinitz and Sharp, 1995]. To date, the experimental possibilities to monitor many regulatory contributions simultaneously are limited. Decomposing these contributions by studying various mutants may only be possible in the most simplistic cases, but even then it is time consuming, and it needs to be considered that mutants by definition express a different regulatory structure and may give false or confusing data. The uniqueness of a mechanism is challenging to identify by studying mutants as well. Regulatory interactions may be direct or indirect so it is not certain, if the observed behavior is due to the mutation or due to unknown downstream effects. To achieve completeness it is certainly crucial to identify all involved parts of a complex system for a general study. Only with a complete set of data it is possible to reconstruct the system and show how the system reacts to different stimuli in a simulation. If the simulated reactions can be validated *in vitro* or even *in vivo*, the hypothesis is that the system was reconstructed correctly. If not, either not all parts or connections were identified correctly. Experimentally dissecting a system is rather challenging as mentioned before: It is often not practical to design *in vitro* or even *in vivo* experiments to obtain the necessary data. It is time-consuming (knock outs), expensive and there is no guarantee of success. Systems Biology can help to overcome these problems by integrating experimental data, modelling and computer simulations to help understanding the relationships among the components of a biological system in order to understand its emergent properties.

1.2.2 Systems Biology concepts

Two main approaches in Systems Biology can be distinguished: top-down and bottom-up.
The *bottom-up* approach: The objective is to gather experimental data about the *system parameters* of a complex system. In the case of a genetic network this would include identifying the genes involved and the formulation of a hypothesis about the interconnection between them. A mathematical model would predict the behavior of the system under defined conditions i.e. how the *state variables* (expression levels in this case) change over time. If the hypothesis is correct, the *in silico* model would predict the same outcome as *in vitro* or *in vivo* experiments would show. Otherwise the model needs adjustments and is usually improved in an iterative way until the predictions comply with the observations (Figure 1.7). One needs to be careful about accepting a hypothesized model prematurely: Even when a model seems to predict the correct answer it is not necessarily correct or complete. Biologic systems are often non intuitive and non-linear - comprehensive testing is required until a model can be considered to be valid.
A recent and very successful example of a bottom-up approach is the reconstruction of the metabolic network of *Mycoplasma pneumonia* [Yus et al., 2009] a human pathogen that causes atypical pneumonia. They used published data available from the Kyoto Encyclopedia of Genes and Genomes (KEGG), data manually obtained from the literature, structural information and homologies to build a comprehensive model of its metabolic network. They validated the constructed metabolic map with 1300 experiments by using defined media of different nutrients. This exhaustive validation gave them a high confidence in their model.
The *top-down* approach requires a precise, usually quantitative, study about the behavior of the system, i.e. measuring the *state variables* at defined timepoints. Depending on the system studied, this is often done by high throughput analysis (to measure concentration and kind of macromolecules) through e.g. microarray expression profiles. Algorithms like ARACNE [Margolin et al., 2006] or CRL [Butte and Kohane, 2000] al-

low building of a hypothesis about the underlying mechanism i.e. reconstructing a gene-regulatory network. The next step usually involves modelling and simulating the hypothesized mechanism and validating the outcome by experimental confirmation of a few selected regulatory relationships, or cross-validation within the training dataset. A true or full experimental validation of the generated networks by these methods has remained elusive due to the lack of a model organism with both a known regulatory structure and compatible experimental data. Dealing with the high degree of complexity of a model, often requires to repeatedly traverse an iterative cycle of revisions and adaptations (Figure 1.7).

Top-down modelling faces challenges when dealing with dynamic processes in living organisms. To date it is not possible to capture the necessary dynamic regulatory interactions experimentally to reconstruct the GAP gene network in early *Drosophila melanogaster*. Yet in [Jaeger et al., 2004] they show a successful example of the *top-down* approach to derive these interactions computationally. The study applied *a priori* knowledge about the involved genes generated in the last 30 years of research, empirically measured and quantified data about protein expression levels and applied a mathematical method called gene circuit to derive data about the regulatory interactions. By employing a heuristic search they minimized the time to find the correct gene - gene interactions out of myriads of possibilities. The result was the first comprehensive description of the gap-gene network and a simulation that helped to clarify direct and indirect interactions in knock-out experiments. With this detailed description it is now possible to study the evolution of this network and compare it to other species like the "moth midge" *Clogmia albupunctata* or the "coffin fly" *Megaselia abdita*.

In this thesis we successfully applied the *top-down* approach [Boehm et al., 2010] to reconstruct the spatial proliferation pattern that would be sufficient to show realistic limb morphogenesis i.e. we inferred a mechanism that shows the correct behavior.

1.2.3 Summary

Systems Biology approaches aim to help us understanding how a biological system is maintained. Classically the methods are applied to study genetic networks and can explain the emerging of a pattern like the segmentation in early *Drosophila* development. The approach offers interesting possibilities to answer developmental questions too: e.g. how growth and adaption are achieved. This system level understanding requires the integration of extensive amounts of data; mathematical, computational, physical and engineering sciences combined help building the required tools to process them. One of the key messages of this thesis is the importance of quantitative data when studying a system and we want to introduce some of the important techniques for this thesis in the next section.

1.3 Quantification of limb development

One part of the thesis is the quantification of the shape geometry of a limb bud to select pairs of limb buds for the modelling approach discussed in the next section. For the modelling it was important to know the time of development between pairs of limb buds. As part of this thesis a morphometric limb staging system - a temporal quantification of limb development - was developed to accurately stage limb buds over a time frame of 36h from mE10:21 to mE12:09.

1.3.1 Staging systems in Developmental Biology

In developmental biology the developmental stage of an embryo is an important measurement. The definition of discrete and well-defined stages made it possible to standardize observations and experimental analysis. Traditionally the gestational age of an embryo (in days or hours) is used for a rough estimate of the developmental stage or where possible the somite count. However, staging systems based on these measures are of limited accuracy because different embryos (even genetically identical ones and littermates) may

not develop synchronously. More refined staging systems were developed and are available for many vertebrates and involve either descriptions covering the whole embryo (C.Elegans, Drosophila, Zebrafish, Xenopus, Chick, Mouse) [Hall, 2008, Jose A. Campos-Ortega, 1993, Hamburger and Hamilton, 1992, Theiler, 1989, Nieuwkoop et al., 1967], or observations of individual organs such as the developing eye, the respiratory system [O'Rahilly, 1983, O'Rahilly and Boyden, 1973] or the developing chick [Saunders, 1948] and the mouse limbs [Wanek et al., 1989].
Staging systems are generally based on qualitative observations of the specimen. The features are either binary descriptions and therefore relatively simple to classify, or the observations are more subtle and usually just meaningful by comparison between two other stages. The main criticisms are the high level of subjectivity and the limited temporal resolution of all qualitative staging systems, such as the Theiler staging for example. Figure 1D in [Boehm et al., 2010] shows 5 limbs of Theiler stage (TS) 19, yet the shape of the limb varies considerably.

1.3.2 Limb-specific staging

Staging systems involving the whole embryo are problematic when dealing with individual organs. Often the amount of synchrony with the rest of the embryo is not known, and the defined stages may not be suitable to discretize the organ development. In Figure 1A [Boehm et al., 2011] , we show the high variability of measurements of the limb buds and the whole embryo of the same gestational ages. Even TS19 staged limb buds show a surprising degree of variability.
A logical step was to focus on the organ of interest when applying a staging system: To our knowledge only the paper by [Wanek et al., 1989] introduced a system for limb-specific staging. Their argument is similar to ours, that relying on the common staging systems is unsatisfactory when the limb is the focus of interest. Since forelimb development precedes that of the hind limb, the limb buds of a single embryo are at different developmental stages. Therefore staging the whole embryo is not precise

enough for differentiating between limb buds. Wanek *et. al.* developed a staging system solely based on the gross changes in the morphology of the mouse limb during its development. Fifteen stages were defined to cover the time from the first appearance of the bud to the completion of limb outgrowth. The stages were defined by several unbiased measurements on the limb, like: width (anterior to posterior), length (proximal-distal dimension), the ratios between them, and other qualitative descriptions.
The use of this staging system is however problematic in the sense of obtaining a) an unbiased stage - as the system relies partly on qualitative descriptions and b) the coarse description of the progressing limb development does not allow for the study of subtle changes in shape and c) the complicated process of measuring the parameters.

1.3.3 The analysis of shapes and Morphometrics

Morphology is the study of gross structures of an organism or taxon and its component parts. It deals with the outward appearance (shape, structure, color and pattern) as well as form and structure of internal parts like bones, organs an muscles. The concept of analyzing a specimen according to these characteristics was first thought of by the German writer and polymath Johann Wolfgang von Goethe in 1802 [Mayr, 1982]. It gradually developed into Morphometrics which is the field concerned with the mathematical quantification of morphology or change in morphology. It removes the need for qualitative description of morphometric features, which allows for a more precise, unbiased and comparable description of size and shape. It became a fundamental part in biological research, especially in paleontology where many other biometric approaches are not feasible [Rohlf, 1990, Gould, 1991]. Several types of morphometrics can be distinguished, each with their own advantages and disadvantages.
Traditional Morphometrics relies on quantitative measurements of features of the specimen: Angles between points of reference, length of structures, weights, numbers etc. which are easy to obtain but may not be biologically meaningful enough for more advanced studies. These measurements were used to assess patterns of variation within and among

samples. Statistical methods like Principal component analysis (PCA), Discriminant function analysis (DFA) or Canonical variates analysis (CVA) were usually employed for ordination and to answer questions like "is there an effect on shape?" and "what is this effect?".
Geometric Morphometrics is considered to be more powerful than traditional approaches: It improves the traditional approach by definition of carefully chosen *landmarks* or outlines and their geometrical relationship to each other to describe the analyzed shape.
Landmarks are ideally homologous anatomical loci that do not alter their topological position relative to other landmarks, provide adequate coverage of the morphology, can be found repeatedly and reliably and lie within the same plane [Zelditch, 2004].
Landmarks are homologous if they are "corresponding" in either biological terms or in functional or developmental terms. Our objective in selecting landmarks is to permit making inferences about the regions between them, rather than the landmarks *per-se*, we are interested in the shapes of the morphological structures on which the points lie. The landmark's role is just to pin down the morphological structure as a discrete point we can identify on all organisms. If now morphological structures between specimens are homologous, discrete points on these structures are as well. Bookstein classified different types of landmarks into three categories: Type I, II and III [Bookstein, 1997]. Type I or A, are unambiguous homologous loci and are considered to be the least problematic type of landmarks. They can easily be found on all specimens and their homology is undoubtable. Examples can be: joints of tissue or bones, juxtapositions of structures, points surrounded by tissue, etc. Type II or B landmarks are points defined by local properties such as extreme-points of curvatures like e.g. the tip of a toe. Type III or C landmarks are also called Pseudo- or Semi-landmarks as they are not real landmarks themselves but can help to describe the shape comprehensively. They are usually defined by their relative or absolute position between other landmarks e.g. "most anterior" or "widest point". Type I and II often do not adequately represent the morphology of interest. Bookstein [Bookstein, 1997] in 2D and Gunz *et. al.* [Gunz et al., 2005] showed that in 3D defining a few

meaningful landmarks on the shape of interest and then placing equally spaced landmarks along the curves or surface can be valuable to complete the description of the shape. Shape differences are usually studied by "homology functions" that describe the deformation from one shape to another (like the "thin-plate spline") or statistical analysis like PCA.
Outline-based methods like eigenshape analysis and Fourier analysis describe a shape with mathematical functions. They have been proposed to capture a shape in more detail and provide a useful tool for the analysis of specimen with few or insufficient landmarks [Lohmann, 1983, Rohlf, 1990, Bookstein et al., 1982, Sheets et al., 2006]. Rather than relying on the definition of landmarks, they require the digitization of the outline of the specimen prior to the analysis. Several digitization approaches can be followed: [Sheets et al., 2006] have studied the use of automated outline tracing based on thresholds of color or contrast to trace the outline of a feather shape. Yet they didn't find this very helpful as the algorithm needed manual correction and no advantage to a purely manual outline tracing could be noted. Their other approach of using a template which is superimposed on top of the digital image to define the points of measurement showed no advantage to a purely manual selection of points of measurement, which also turned out to be less time consuming in their study. The dense number of sampling points was reduced by a linear interpolation to obtain a fixed number of equally spaced points. This Semi-Landmark based way of quantifying a shape [Bookstein, 1997] requires further alignment of the selected semi-landmark points to reduce the effect of the arbitrary selection of a limited number of points along the outline.
Alignment approaches: Several methods for superimpositions have been proposed and can be used to remove the influence of location, rotation and if desired, scale. An early and rather simple approach is Two-point registration [Zelditch, 2004] but more popular is the Generalized Procrustes superimposition. In this approach an initial reference shape is selected randomly for the dataset and the centroid of this shape is fixed at the origin of the coordinate system. The next (optional) step is to rescale the shape to a unit centroid size. The other shapes are processed in the

same matter and are aligned to the reference shape by rotating to minimize the summed squared distances between homologous landmarks (the Procrustes distance). After all shapes are aligned a mean form for the analyzed specimen is estimated and the other shapes are realigned to this new reference shape. This process is done iteratively until the current mean shape is the same as the previous (which usually happens after a few iterations) [Rohlf, 1990]. An optional step to improve the achieved alignment is to adjust the positions of the landmarks - the tangent to the curve at each landmark point is estimated and the landmark is allowed to move along this tangent. Where *bending energy minimization* tries to achieve the smoothest possible deformation from the analyzed to the reference form, *perpendicular projection* tries to remove all variation tangents to the curve. Both methods appear to perform equally well [Sheets et al., 2006].
The aligned shapes are further compared by a suitable ordination method. Elliptical Fourier analysis (EFA) [Kuhl and Giardina, 1982] is a Fourier decomposition method usually used for dimensionality reduction of morphometric data. In a two-dimensional case the increment in x and y coordinates around the outline of a specimen defines a periodic function which can be decomposed by a Fourier expansion into terms of sine and cosine curves of integer frequencies with appropriate amplitudes. The number of decompositions (harmonics) influences how well the shape is approximated and how well it can be reconstructed for visualization purposes. In Ferson *et. al.* they showed the condensation of 450 trace coordinates into 40 Fourier coefficients while maintaining enough shape information to recreate the original shape in an acceptable way [Ferson et al., 1985]. The obtained Fourier coefficient then may be subject to further statistical analysis like PCA, DFA or CVA for ordination. Like most outline-based approaches, EFA requires alignment of the outline shapes to determine homologous points of comparison.
Eigenshape analysis is a procedure to assess shapes according to their similarities and differences in their outline-shape. Eigenshape analysis identifies the minimum number of shape functions that adequately represents a collection of shapes. The method is designed to discriminate against subtle, complex and continuous changes in shape, which are the

most difficult to evaluate by eye. Therefore it essentially derives orthogonal shape functions by an eigenfunction or principal component analysis of a correlation matrix between shapes. Like all outline-based methods it requires the digitization of shape into a set of Cartesian coordinates. These are usually converted by the ϕ shape function of Zhan and Roskies to calculate the net angular deviation between the chords connecting adjacent landmark points [Zhan and Roskies, 1972]. The next step involves the alignment of the shapes to be analyzed. In the case of analyzing multiple shapes a similar approach to the generalized Procrustes analysis is used, where one randomly selected shape acts as a reference shape and the other shapes from the dataset are aligned with respect to it. To ensure a meaningful point-to-point comparison between shapes, the outline perimeters need to be interpolated to the same number of equal distant segments before computing the normalized form. The shape functions usually show a high but varying degree of similarity so most of the shape difference can be represented as linear combinations of just a few uncorrelated shape functions. Once the shape functions for the dataset have been determined they are submitted to a singular value decomposition [Reyment and Jöreskog, 1996] using the pairwise correlation or covariance matrix as a basis for the quantification of shape similarities. The results are (a) equations for the principal- or eigenshape-axes (b) a set of eigenvectors for each axis (c) scores for the shapes and the eigenshape functions. The first eigenshape (ES_1) represents a function for the standard shape derived from the dataset - this modelling capabilities are considered one of the main strength of eigenshape analysis. The score for the first eigenshape axis is a constant multiplied with each term in the shape function associated with the first eigenshape. It results in purely angular change of the shape and the mean score of objects on this axis results in a very close approximation of the sample mean shape. Subsequently (ES_2..ES_n) have a mean score resembling variations around the means shape.

Ordination is the process of describing the diversity of shapes in a sample. The most simplistic approach is to describe difference as the distance between the coordinates of corresponding landmarks. These can be used as

they are or be further processed by multivariate statistical approaches like PCA [Pearson, 1901], CVA, DFA or classifying specimen based on maximum likelihood. The main purpose of these tools is to simplify the description of the shape to be able to find answers to the relevant questions e.g. how the shapes differ. PCA is suitable to simplify the description between individual shapes and CVA is used to quantify the differences among groups of shapes. Both methods transform the initial set of shape variables into a new (smaller) set of variables that are linear combinations of the original ones. The underlying concept is that geometric shape variables are neither biological nor statistically independent because they describe features in the specimen that are functionally, developmentally or genetically linked. PCA is useful to simplify the often complex and hard-to-interpret patterns of variation by replacing the original variables by new variables - the Principal component (PC). The first PC describes the largest possible portion of variance, PC2 the next largest portion of variance which is not yet described by PC1 and so on. Usually a few PC explain most of the variance in shape, making the presentation of the results more easily understandable. They also produce scores for individuals on those PCs and the specimen can be ordered according to theses scores. One of the ideas of PC is to reveal patterns that may show biological relevance. CVA follows the same principles but allows for the quantification among groups of specimens.

1.3.4 Generating a 3D Shape

For our modelling approach, using a FEM simulation we need to define the geometric domain for the problem. This requires first the definition of a surface mesh and then discretization of the covered space. Such a surface can be obtained by manually drawing it in a 3D software (various CAD or 3D animation programs are available for this purpose) or by a mathematical definition of the surface. Real-world objects can be digitized by 3D scanners on various scales. The purpose of a 3D scanner is usually the generation of a point cloud of geometric samples of the surface of the scanned object. The surface of the object can be

extrapolated or reconstructed from this data source. On a macroscopic level various types of Laser-scanners can be used to probe the surface of an object. Magnet Resonance Imaging (MRI) or X-ray Computed Tomography (CT) can go a step further and also penetrate the inside and generate a voxel (3D pixel) representation of an object. Mouse embryos lie on a mesoscopic level (between micro- and macroscopic) where micro-CT or Optical Projection Tomography (OPT) [Sharpe et al., 2002] can be used to scan small objects and reconstruct the surface. OPT was especially designed in our lab to generate full body penetrating 3D images of object on a mesoscopic scale and was ideally suited to obtain geometric information of mouse embryos. On a microscopic scale confocal and recently SPIM microscopy can be applied for 3D imaging.

1.3.5 Quantification of cell proliferation

In 1970 Hornbruch and Wolpert [Hornbruch and Wolpert, 1970] reported a gradient in cellular proliferation in the chick limb at Hamburger&Hamilton stages HH23-27. They discovered the gradient of distal-high vs. proximal low proliferation by analyzing the mitotic index of mesenchymal cells by haematoxylin and eosin staining. More recently [Fernandez-Teran et al., 2006] studied the cell proliferation activity in the mouse and chick limbs in more detail by using anti-Phosphorylated-histone H3 (pH3) immunohistochemistry and Bromodeoxyuridine (BrdU) staining and found a similar general pattern for these stages. However, single labelling techniques like these have an important limitation. Determining the number of cells in one cell cycle phase as a fraction of the total number of cells (for example the proportion of BrdU-labelled cells in S-phase) is a relative measurement and cannot provide information on how long that phase lasts in minutes or hours. This limitation applies to all single-labelling approaches, whether using BrdU, pH3, or tritiated-thymidine. Previous studies have therefore provided information on the relative rates across different regions of the limb, but did not aim to quantify these spatial patterns in terms of cell cycle time.

Pulse-chase experiments overcome this limitation through the use of two or more labels administered to the living cells at different times [Dolbeare et al., 1983]; however, this has typically been done on dissociated cell populations analyzed by high throughput techniques, thereby losing all spatial information. A double-labelling technique was successfully used by [Martynoga et al., 2005] to quantify proliferation rates on 2D sections of the developing telencephalon. They measured the cell cycle times by sequentially staining the proliferating cells with two different markers BrdU and Iododeoxyuridine (IddU) at a known time interval and thereby creating a new artificial phase of the cell cycle whose exact duration is known whilst maintaining the spatial arrangement of cells.

1.3.6 Summary

Staging is a technique to track and follow the development of a developing biological system. Most systems consider the whole embryo and are based on qualitative descriptions to distinguish between stages. Few unambiguous staging methods based on quantitative measurements exist and the development of a new system was required to achieve a satisfying temporal resolution. Morphometrics describes the methods to quantify a landmark free shape - the limb bud. A staging system can be based on these methods.
Quantification of the shape geometry of a limb bud can be performed by OPT which was especially designed to scan specimen of the size of an embryo in 3D. The quantification of cell proliferation rates while retaining the spatial information was shown by a pulse chase double-labelling technique with BrdU and IddU.

1.4 Modelling

The Systems Biology approach followed in this thesis comprehends the formulation of a model of growth and integrating the quantified data. A simulation using this model shows if the underlying hypothesis was cor-

rect. Modelling and simulating belongs to the most important tools of Systems Biology to test a hypothesis. This section introduces some of the concepts in science of formulating a model and simulating it.

1.4.1 Modelling and simulations in science

Modelling is the process of reproducing one part of reality to improve our understanding of it and sometimes to make predictions about its future conditions. Modelling intentionally neglects certain aspects of reality, simplifies others and is usually tailored to answer a specific question. Despite this intrinsic weakness, models are extremely useful, and disputing models is fundamental to the scientific community.
One of many uses of models is to generate data where the use of experiments is either impossible or impractical. The results obtained strongly depend on the assumptions that lead to the model.
Modelling became one of the major tools for systems biology and many software tools such as E-Cell, Gepasi, Jarnac, StochSim, The Virtual Cell, CompuCell3D etc. have been developed to build, test and improve models
A data exchange format Systems Biology Markup Language (SBML) was invented to store developed models, share them and enable the use of different software tools without rewriting code. Public databases store such models in SBML format and make them publicly available (e.g. BioModels [Le Novère et al., 2006]).
A *simulation* is the implementation of a model, where we distinguish steady state simulations which provide information about a time-invariant system and dynamic simulations providing information over time. The purpose of a simulation is to test and analyze a model for its accuracy and completeness. If the predictions of a simulation are consistent with empirical results and explain past and future observations, the hypothesis is that the model is valid. Towards the formulation of a model for limb bud outgrowth and parameterizing it, we need to understand the physical properties of the mesenchymal tissue.

1.4.2 Modelling the mechanics of biological tissue

In this study we analyzed the developmental stages mE10:15 and mE11:00, where the limb is composed of uniform mesenchymal cell covered by a layer of ectoderm. The physical properties of mesenchymal tissue was analyzed in a classical study by [Phillips et al., 1977] where he reported that the tissue behaves like an elastic solid over very short time scales but displays a liquid-like characteristic in response to stress in long-term culture. The time scale of development we wished to model was 6h, where the tissue has liquid like characteristics. The motion of a fluid is a problem described by the Navier-Stokes equations [Navier, 1822], mostly applied in the engineering field of fluid dynamics to study the properties of liquids and gases as functions of space and time. More precisely, they describe the balance of forces acting at any given region of the fluid (a velocity field or flow field). In a previous study by Dillon&Othmer, a limb development simulation in 2D employed the Navier-Stokes equations to represent the mesenchyme as a viscous incompressible fluid whose volume increases corresponding to a distributed source term, **s**, which represents the patterns of growth [Dillon and Othmer, 1999]. They used FEM, a tool of Computational Fluid Dynamics (CFD), to simulate the behavior of the limb.
CFD is the part of fluid mechanics using numerical methods and algorithms to analyze and solve problems that involve fluid flows. CFD is state of the art for solving fluid dynamic problems and involves an initial definition of the geometry where the problem is analyzed. Then, a set of differential equations is solved over this domain, which describes the motion of the fluid and the generated stresses. FEM is the most popular way to solve these equations and in line with Dillon&Othmers study, chosen for our model of growth.

1.4.3 Finite Element Modelling

The FEM technique is a numerical method to approximate solutions to differential equations that model problems in physics, engineering or in

fluid dynamics. It requires the problem to be defined in a geometrical domain, divided into a finite number of sub-domains. By "meshing" the domain, we can obtain triangles or quadrilaterals in a 2D case or tetrahedrons and hexahedrons for 3D problems. Over each of these elements the unknown variable (pressure, velocity, temperature ...) is approximated as being constant and described by a function such as the Navier-Stokes equations. Since the first formulation [Clough, 1960] it has developed into a standard method for numerical approximations of the Partial differential equation (PDE) defining engineering and scientific problems [Pepper and Heinrich, 1992].

1.4.4 Meshing a 2D or 3D Shape

After generating the 3D surface or the 2D shape, the next step towards FEM is the meshing of the geometric domain. Meshing is the process of discretization of the previously extracted shape geometry into small elements or cells. It can be approached in many different ways:
In most cases the geometry describes the edges of an object in a 2D case or the surface in a 3D case (Figure 1.8), which is subsequently meshed. A suitable mesh for FEM needs to meet certain quality-standards which may vary for different problems. A rule of thumb would be that a mesh is good if the FEM simulation shows a high numerical stability, for each step of the simulation an error estimate is calculated to measure how stable the solution is. A good mesh leads to the best numerical accuracy i.e. the least approximated error. Though this error can't be known *a priori*; a few criteria are common to most meshing processes:

- The mesh should be smooth without abrupt changes in the geometry.
- Internal angles of triangular meshes should be close to 60^o and quadrilateral meshes should have approximately 90^o angles.
- Variation in edge length should be minimized.

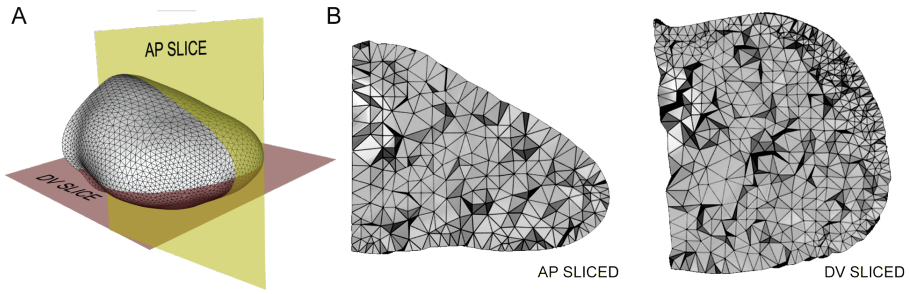

Figure 1.8: **Examples of surface and tetrahedralized meshes.**
(A) The surface mesh reconstructed from scanning a limb bud by OPT (B) the same scan fully tetrahedralized by NetGen and sliced at the AP and DV axis showing the interior tetrahedra.

- The mesh should contain enough elements to achieve an acceptable degree of accuracy with least computational costs.
- The mesh should be smoothly refined in the areas where the geometry changes rapidly.
- Some artifacts that usually render the mesh unsuitable for most simulations should be generally avoided: Mesh folding, Cells with negative Jacobian values, bow-tie elements, non-convex elements, extreme variation in edge length, variation in included angles, changes in cell size etc.

Most PDE solvers offer a graphical representation of the approximated solution. Even if no error estimate is calculated numerical problems show usually visually by an obvious disintegration of the mesh geometry (Figure 1.9) as a result of the simulation. Applying these criteria leads to a satisfying result in most cases, however there are more sophisticated and objective mathematical approaches mentioned in [Frey and George, 2000] chapter 18. They include the adaptive refinement of the mesh and the reduction if the timestepping i.e. how

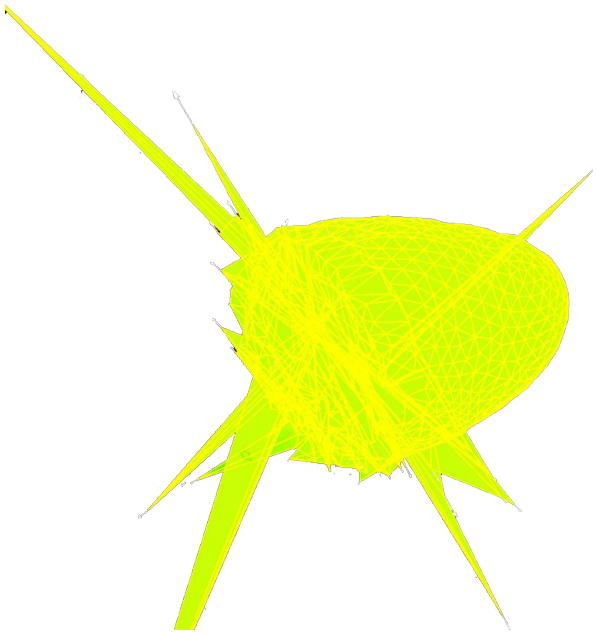

Figure 1.9: **Disintegrated Mesh.**
Numerical problems often show in a disintegration of the mesh geometry.

many simulations are performed for a simulated period of time. These methods are valuable in critical applications of engineering problems and are beyond the scope of this thesis.
Mesh creation is usually done semi-automatically by a suitable software tool that applies one or several of the standard algorithms such as:

- Quad-/Octree-based spatial decomposition methods have been designed to meet the needs of automated mesh generation of arbitrary objects without the need of manually post-processing [Shephard and Yerry, 1983, Shephard et al., 1988, Thacker, 1980].
- The Advancing Front technique is based on the pioneering work of [George, 1971] which was extended by [Lo, 1985] and [Peraire et al., 1987] until the currently mostly used formulation of [Shostko and Löhner, 1995] into a powerful meshing technique dealing with arbitrary shapes in 2D and 3D.
- Delaunay-based triangulation started with the pioneering work of Delaunay himself [Delaunay, 1934] and was further improved by many researchers since. Among them are [Preparata and Shamos, 1985, Rajan, 1994, Ruppert, 1995].

In our case of generating a 3D mesh of a limb bud, we employed OPT for scanning. A filtered back-projection algorithm to reconstruct the surface and NetGen [Schöberl, 1997] an open source meshing tool using the "advancing front" algorithm to produce high quality meshes for FEM.

1.4.5 Reverse engineering

The last concept that should be mentioned here is "reverse engineering", a method that was applied in this thesis to derive a hypothetical proliferation pattern that would show realistic growth in agreement with empirical measurements about outgrowth.
When empirical data can't be obtained directly or not on a sufficiently detailed level, this strategy can be used to generate data to test a model. The

phrase was adopted from the field of engineering, where it describes the process of discovering the technological and mechanistical principles behind a man-made object. Its purpose is to reproduce the original without knowing the procedures and ideas involved in the process of its creation. Also in software engineering, reverse engineering is used to understand the principles of a compiled program. It is often used for hacking or bypassing copy protection mechanisms (e.g. the tool DeCSS to decrypt the content of a movie DVD) or analyzing malware code like the recent StuxNet Worm believed to be tailored to attack a specific infrastructure.
In biology, reverse engineering describes the process of estimating the required variables and/or their values to simulate the behavior of a biological system. For the typical Systems Biology problems such as network reconstruction from high throughput data, machine learning algorithms like ARACNE [Margolin et al., 2006] Bayesian networks and CRL [Butte and Kohane, 2000] are mostly used. Dynamic interactions between components or concentration levels of the system have successfully been reverse engineered by parameter optimization strategies [Jaeger et al., 2004]. The dynamic cell proliferation during limb development forms a comparable problem we sought to study likewise.

1.4.6 Parameter optimization

The concept of parameter optimization can be pictured through the idea of a fitness landscape (by analogy with a real mountain landscape with valleys and hilltops). The full space of the landscape represents the full range of parameter combinations for the model, and the height of the landscape at any given position represents the fitness of those particular parameters (i.e. how good this particular solution is). An optimization algorithm determines the fitness of a given point by performing a simulation with those parameter values and assessing the solution by a problem-specific fitness function. A comprehensive survey of the whole landscape can be problematic as it usually turns out to be too computationally expensive (millions of simulations would have to be performed). The goal of an optimization method is therefore to find the best solution by a series

of carefully-selected simulations, thereby "intelligently" selecting a path through the landscape towards the higher mountains or deeper valleys.
In general, two classes of optimization methods are distinguished: local and global: Global search methods are useful when the search space is likely to have many valleys and hilltops (known as a rugged landscape), making it hard to locate the true global optimum. They are mostly of a stochastic nature to prevent getting trapped in local optima, however they might not find an optimal solution in a feasible amount of time (for example Simulated Annealing [Kirkpatrick et al., 1983]). Local optimization methods by contrast can be used for either low dimensional or constrained problems (known as a correlated fitness landscape). Local methods start from a specific initial set of parameter values (i.e. an initial position in the landscape) and assume that a continuous "uphill" path leads to the global optimum. They try to improve the current best solution by searching in the direct neighborhood for a better solution candidate. Usually they converge quickly to a solution. By their nature, local search algorithms are typically incomplete as the search may stop before best solution was found. This happens if the algorithm is trapped in a local optima where each neighboring solution is worse than the current candidate but the true best solution lies far apart. The choice of which method to use strongly depends on the problem and needs to be sought carefully [Ashyraliyev et al., 2009].

1.4.7 Summary

Building the model of a mechanism and running a simulation can be useful methods to test a hypothesis. To have biological relevance the parameters of the simulation should base on empirical measurements. Where this is not the possible a "reverse" approach can be followed. Empirical measurements of the behavior of the biological system allow for "reverse engineering" the underlying mechanism. This mechanism could be a genetic network like the gap gene network, or the spatial proliferation pattern in the limb bud.

1.5 Summary

In this thesis we follow the Systems Biology approach of quantification and modelling to test a popular hypothesis about the cellular mechanisms promoting limb elongation. This approach requires quantitative data about limb development and a model to test the hypothesis. The goal is to formulate a data-driven simulation of outgrowth and the comparison of the simulated results with experimental data.
By this quantification of time we selected two sets of limb buds that are 6h of development apart from each other which served as models to test the hypothesis of "growth-based morphogenesis" We quantified these limb shapes by 3D scanning with OPT as well as the spatial cellular proliferation pattern in limb buds of the chosen developmental stages. The quantified shapes and the spatial proliferation pattern were used as realistic input into a computer simulation to predict the change in morphology. After showing, that a realistic change of shape can't be achieved with the measured proliferation pattern we developed a parallelized parameter optimization running simultaneously on 200 nodes of a computer cluster. With this powerful technique, we computationally derived a proliferation pattern that promoted realistic outgrowth. This way we could estimate if the first simulation failed because of measurement errors or if "growth-based morphology" is indeed not a realistic hypothesis.

Chapter 2

OBJECTIVES

The previous chapter has extensively discussed the limb as a model system. Great strides have been made to increase our understanding of the molecular processes involved in its formation, patterning and morphology. Yet the cellular behaviors were rather neglected in comparison and little is known about them. A popular hypothesis states that a graded cell-proliferation increasing distal to proximal is the driving force behind limb outgrowth. Main objective of this thesis is to test this hypothesis for its plausibility by a data-driven computer simulation and suggest alternatives.
They can be summarized as follows:

1. Development of a data-driven computer simulation, incorporating quantitative measurements about limb age, geometry and spatial proliferation.

2. Development of a staging system standardizing limb development to relate limb buds at specific time points to a particular stage of development and especially detect the age different between pairs of limb buds.

3. Building a quantitative map for the proliferation pattern of the limb bud for two selected developmental stages.

4. Building a quantitative 3D representation of the limb shape geometry suitable for Finite element modelling (FEM).

5. Building a dynamic model of growth to study the implications of different spatial cell proliferation patterns on limb morphogenesis.

6. Reverse engineering of a proliferation pattern that will be able to reproduce empirically measured development and compare the pattern to the previously measured to make statements about its plausibility.

Chapter 3

THESIS PUBLICATIONS

3.1 A landmark-free morphometric staging system for the mouse limb bud

Boehm B, Rautschka M, Quintana L, Raspopovic J, Jan Z, Sharpe J. A landmark-free morphometric staging system for the mouse limb bud. Development. 2011; 138: 1227-1234.

3.1.1 Additional Methods

Size independent sampling of the outline

To compensate for the lack of size information if no pixelsize value is provided, we sought of a different way to sample the spline in a sequence of equal distant points: For each controlpoint placed by the user along the outline, the system creates 20 equally-spaced semi-landmarks. In line with the generalized procrustes analysis we linearly interpolate (stretch or un-stretch) this vector to match the number of elements of the standard limb. Further we align the two shapes and allow for a correction of the interpolation by +/- 20%, working out how many elements the "overhanging" regions contain. In our test the users did not draw more than 20% dispensable shape information so this limitation was chosen to reduce the computational expenses.
To study how much the size influences the staging result we also implemented a "semi size-independent" version where pixelsize information is used for the calculation of equal distant semi landmarks but then proceeds with the previously explained scale free comparison method (pixelsize-dependent, scale-free).

Normalization of the score between shapes

The size dependent comparison method requires the normalization of the genuine difference scores between shapes: As size is included in the shape information and the semi-landmark points are sampled at equal distances of 20μm, the number of semi-landmark points increases with age. And so will the score proportionally i.e. comparing a young limb with a young standard shape will give a lower score whereas comparing an old limb bud with an old limb bud shape will result in a proportionally higher, albeit both show a similar match. This causes the problem that especially older limbs are staged too young as younger limbs contain less elements. To compensate for this we divide the score by the sum of the total gradients for the vector at each semi-landmark point which linearly increases the more older and more complex the shape gets.

3.1.2 Supplementary figures

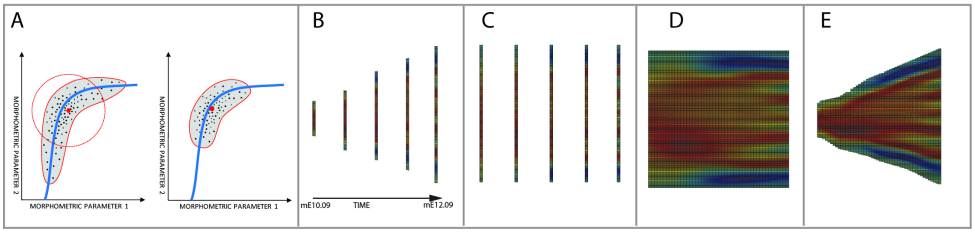

Figure 3.1: **Strategies to create the standard trajectory**
(A) A schematic representation shape space for all limb buds harvested at a single timepoint. Averaging these shapes would not necessarily give the right representation for this timepoint. Our approach removes outliers that are more likely to be older or younger than the real average age. The curvature graphs of the standard limb buds (B) are stretched to equal lengths (C) To fill in the 12 hour gaps new shape data in one hour steps was interpolated. (E) The curvature graphs were stretched back to their original size.

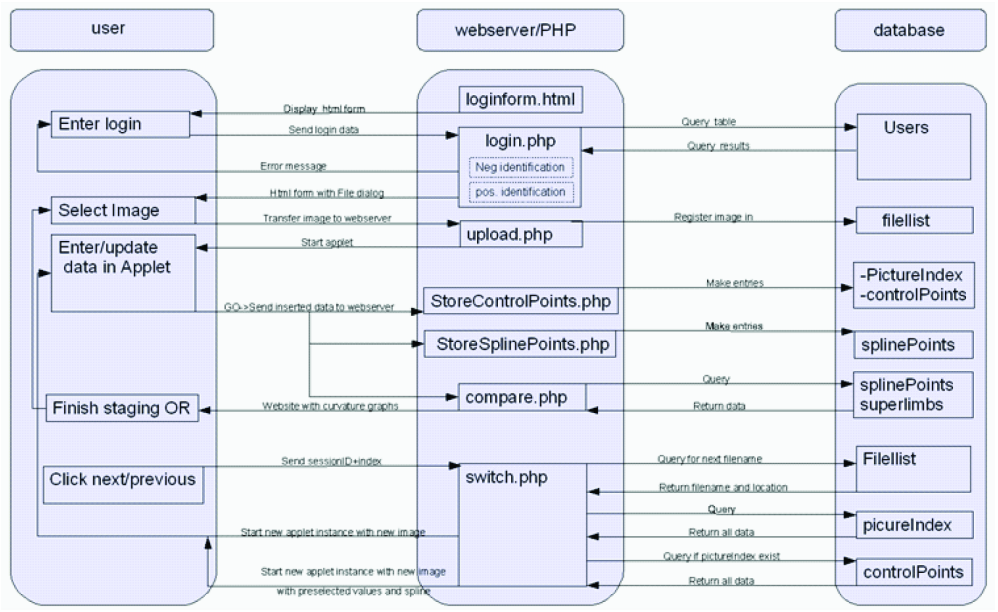

Figure 3.2: **Schematic view of the staging software.**
This diagram shows how the font-end, back-end and the database of the staging software interact, as well as the general architectures of the staging system.

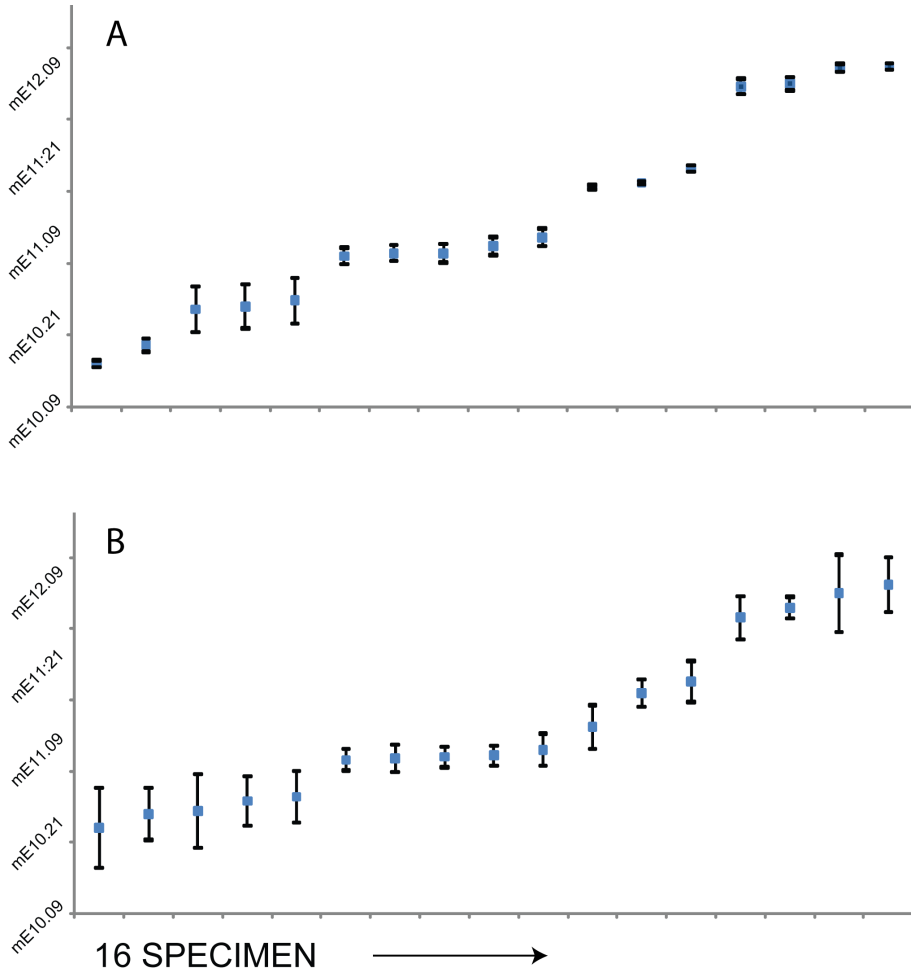

Figure 3.3: **User test of the scale free staging system.**
The same data of the previous test by 5 users with 16 different limbs was (A) analyzed with the scale free version of the staging system that included the pixelsize for spline segmentation. The overall staging stays consistent, however the variation increases to +/- 3 hours between users and the σ increases to 116 min. (B) the scale free version without pixelsize information performs worse with a σ of 360 min.

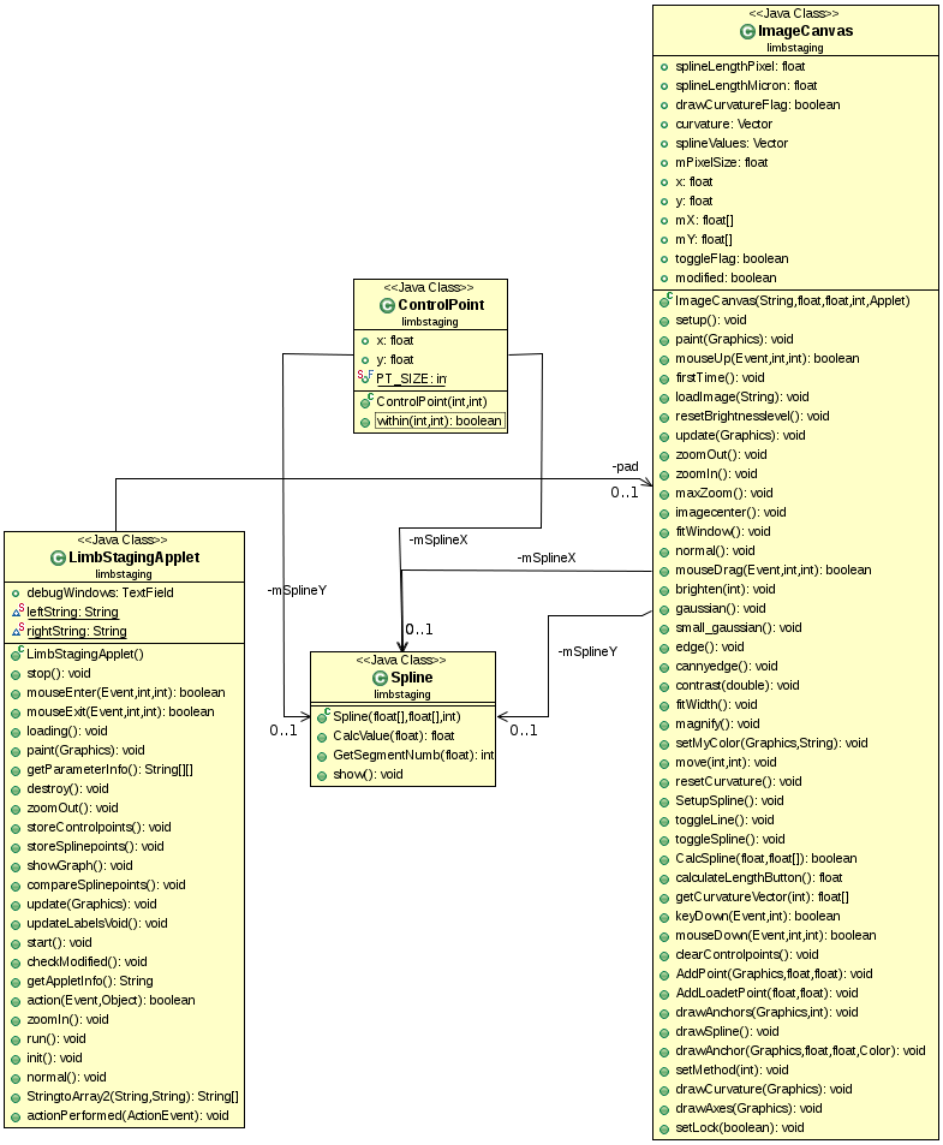

Figure 3.4: **Class-diagram of the staging applet software**
The frontend was developed as a Java Applet (Java 1.6.20). It can be used on most platforms where a browser with the Java Applet plugin is available. It was positively tested under: Windows XP, Vista, 7; Mac OS-X; Linux. The database connection was realized by PHP5 and JSON as data exchange format.

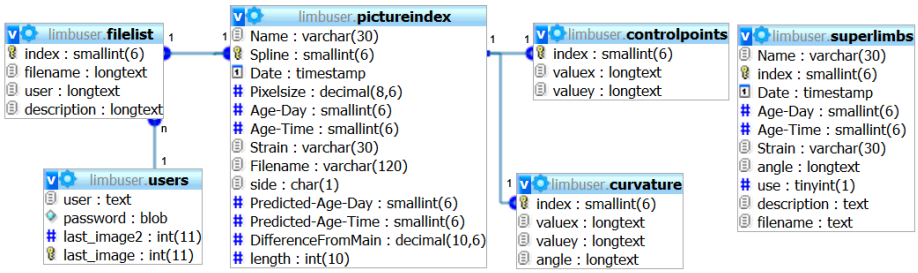

Figure 3.5: **Database schema of the staging system**
For every image we create a new database entry, including the filename, gestational age (if known), pixelsize (if known), the controlpoints along the limb shape, some free text describing the image, information if it is a left- or right hind limb - after staging the predicted stage is added. Each image can be related to a specific user, creating a browsable list by in the staging applet.

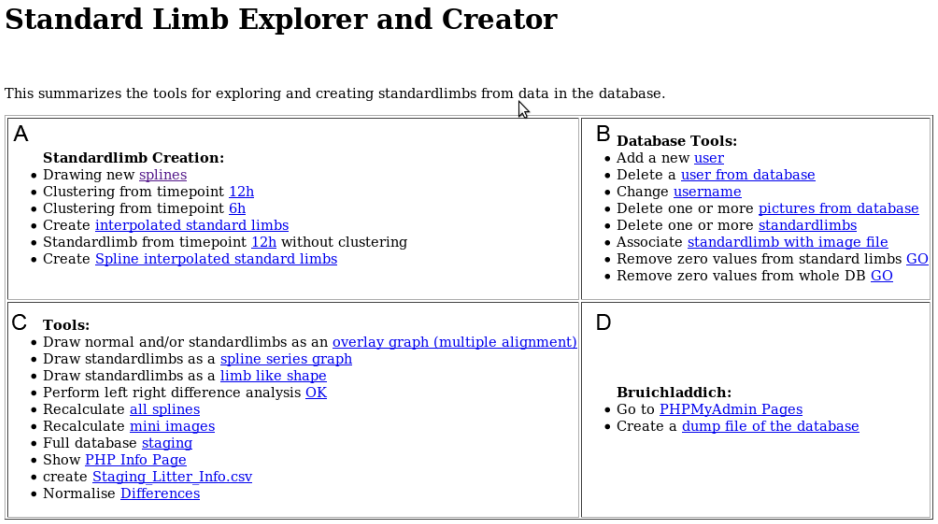

Figure 3.6: **Administration view of the staging system**
Extensive amounts of source code were written to contribute to this project, a schematic view of the administration console of the staging system points out some of the most important methods. (A) The tools to create the standard trajectory, including: Calling the Applet, selection of a sub-sample of the primary timepoints and merging it into a standard shape like described in Figure 3.1, selection of a subsample to refine the resolution to create real timepoints 6h apart - not successful, a linear interpolation to increase the temporal resolution, a tool to merge a selected set of limb shapes, a spline interpolation between the primary timepoints to increase the resolution.

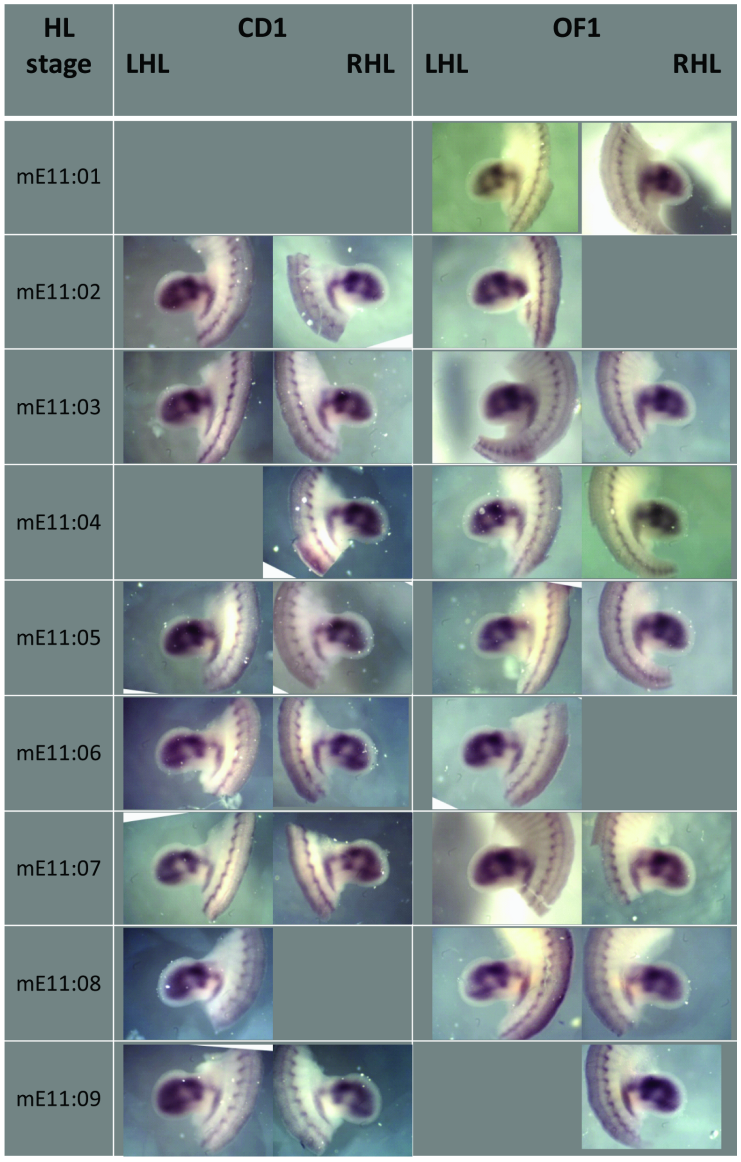

Figure 3.7: **Additionally 100 WMISH for Sox9 Part I**

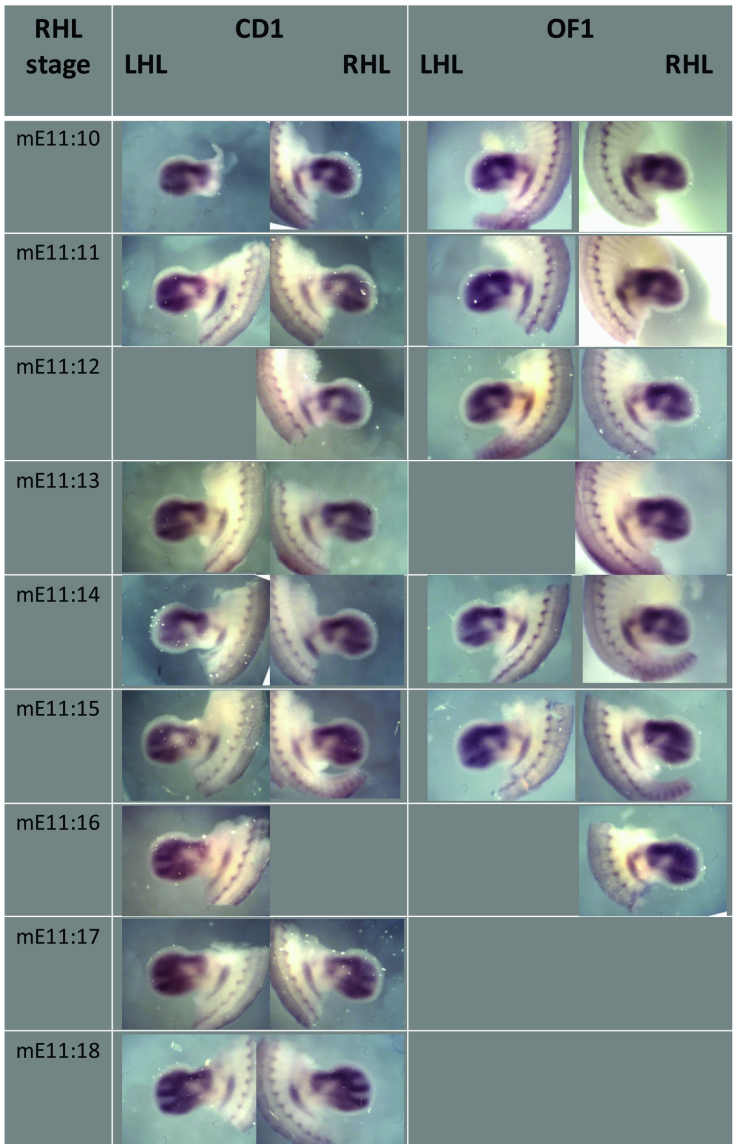

Figure 3.8: **Additionally 100 WMISH for Sox9 Part II**
We performed additionally 100 WMISH and here we show 58 images of two different mouse strains (OF1 and CD-1). By ordering the images according to their morphometric stage we show a time coarse covering 17 hours of development. We can follow the subtle changes in the expression of Sox9 and compare them in the two different strains. However the strains differ in size the Sox9 pattern is comparable between equal stages with a slight delay in the pattern of OF1.

3.2 The Role of Spatially Controlled Cell Proliferation in Limb Bud Morphogenesis

Boehm B, Westerberg H, Lesnicar-Pucko G, Raja S, Rautschka M, Cotterell J, et al. The role of spatially controlled cell proliferation in limb bud morphogenesis. PLoS Biol. 2010; 8(7): e1000420.

3.2.1 Supplementary figures

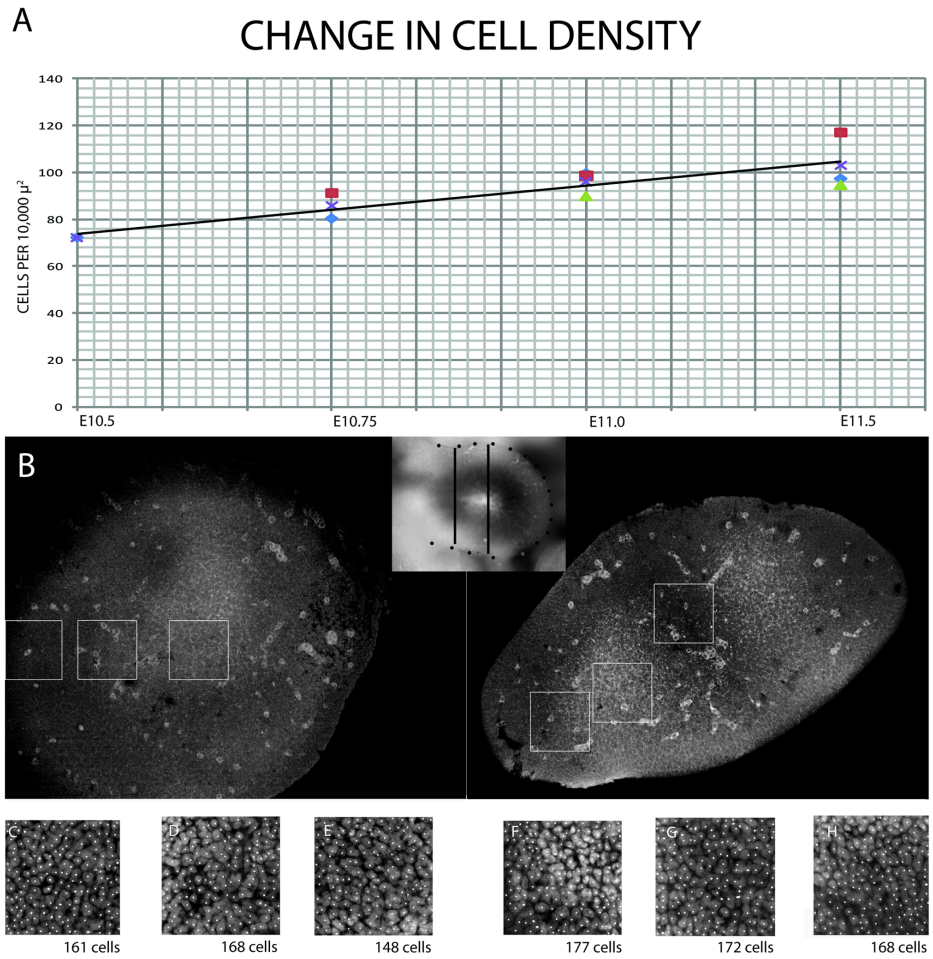

Figure 3.9: **Analysis of mesenchymal cell density.**
(A) Graph of cell density against age of hindlimb bud. The two simulations in the paper correspond to the first and last third of this plot (E10.5-E10.75 and E11.0-E11.25). From this graph we calculated the density increases of 2.1% per hour for the younger, and 1.7% per hour for the older interval. (B) A limb bud of E11.25 was fluorescently-stained for Sox9 expression. Two sections were imaged under two different

fluorescent channels - the upper row shows only Sox9 expression (see [Hecksher-Sorensen and Sharpe, 2001] for technical details). The inset panel illustrates where these sections lie on a photo of another WMISH for the same gene. (C-H) The lower row of square panels displays sub-regions from the two sections (positions shown as white squares in (B), in which only the fluorescent nuclear label is shown. In this way we were able to compare the cell density from Sox9-expressing regions (pre-skeletal) with the non Sox9 expressing mesenchyme. The cell counts show there is no obvious sign of mesenchymal condensation yet, despite the expression of Sox9.

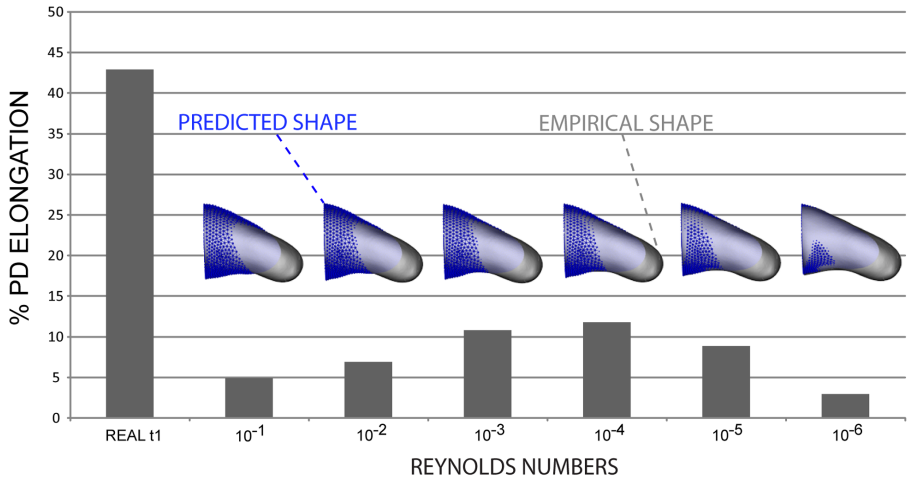

Figure 3.10: **Effect of the Reynolds number on the simulations.** The resulting shapes of the simulation with 5 orders of magnitude difference in the Re number were compared. The measured PD elongation varies between 3% and 12%, whereas the real elongation is 43%.

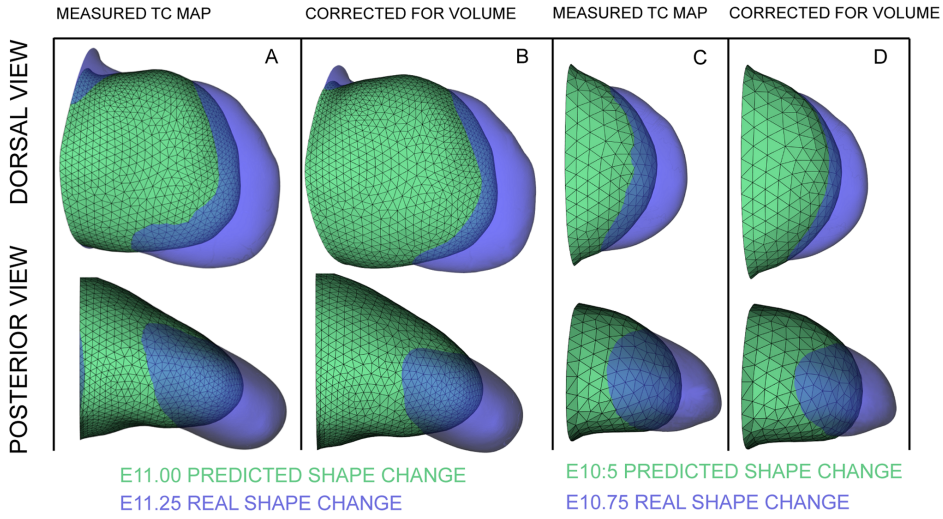

Figure 3.11: **Volume-corrected simulations.**
(A) The predicted shape change achieved with the cell-cycle times obtained by experimental data (as in Figure 4D). (B) Simulation in which the Tc values were scaled-up to create the correct volume for the real t1 shape, proving that this correction does not improve the final predicted shape - the predicted and real t1 shapes still fail to match. (C-D) The same result for the E10.5 simulation.

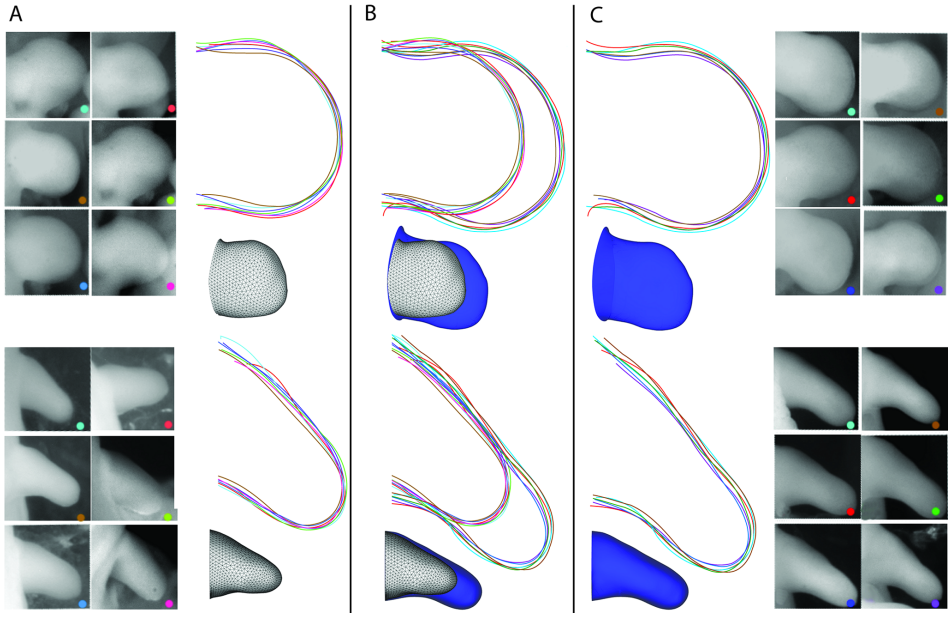

Figure 3.12: **Reproducibility of limb Shapes.**
Since the assessment of simulations depends on detailed shape information from 2 different specimens (for St_0 and St_1), it is important to confirm the general reproducibility of mouse limb bud shapes. (A) Six limb buds were chosen at stage E11.0. By extracting the outline of each limb (both from a dorsal view and a posterior view) we can overlay them to illustrate the minimal degree of shape variation. (C) The same data was obtained for limb buds 6 hours older (E11.25). (B) By overlaying the 2 ages, we can confirm that the developmental shape change between the two stages is large by comparison with the variation within each group.

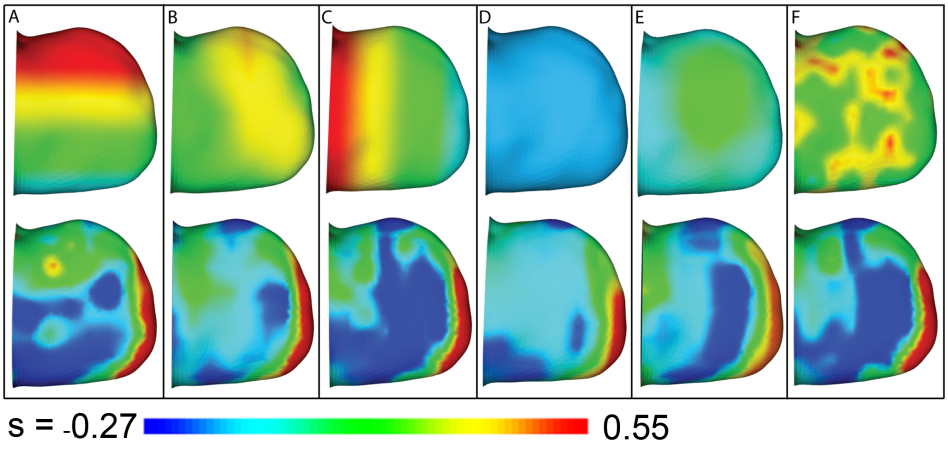

Figure 3.13: **Fitness Landscape Analysis.**
The reliability of the parameter optimization was assessed by starting from 6 different initial proliferation patterns. These patterns were not chosen randomly but specifically represent extreme alternative spatial distributions. The results show that, despite the dramatically different initial conditions, the algorithm always converges at a similar solution. All panels consist of a ventral view showing the initial proliferation pattern (top) and the optimized result (bottom). The following initial patterns were used: (A) AP-graded proliferation pattern with highest values on the anterior side, (B) a radial pattern with a central core of high proliferation, (C) high proliferation proximal and low values distal - this is the inverse of the optimized pattern, so requires a complete reversal of the pattern, (D) uniform zero proliferation, (E) a core of low proliferation in the center of the limb and high values nearer the ectoderm, and (F) a random spatial pattern.

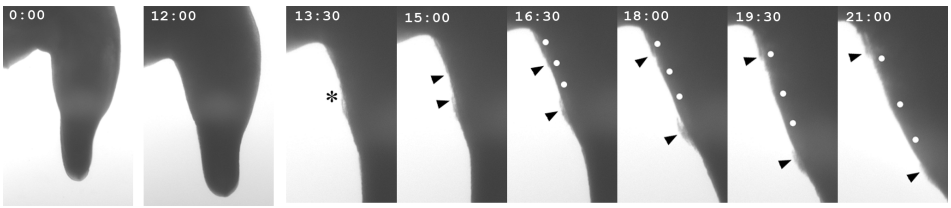

Figure 3.14: **Mesenchymal movements in the absence of overlying ectoderm.**
An E12 mouse limb bud was cultured in-vitro for time-lapse imaging (see [Boot et al., 2008] for more technical details). After the initial adjustment phase, the limb bud shape changes were quite normal (although as usual for in-vitro culture growth was slower than in-utero). After about 12 hours a tear appeared in the ventral ectoderm. This is highlighted at 13:30 with the asterisk. In the subsequent frames (every 1.5 hours) the damaged edges of ectoderm can be seen slowly pulling away from each other (black arrowheads), revealing the mesenchyme underneath. Visual contrast in the mesenchymal tissue allowed us to track the positions of 3 points of tissue (white dots) over the remaining 11 hours. These frames show that the living, growing mesenchyme does not spill out into the medium and instead continues to actively expand parallel to the PD axis, despite the absence of overlying ectoderm.

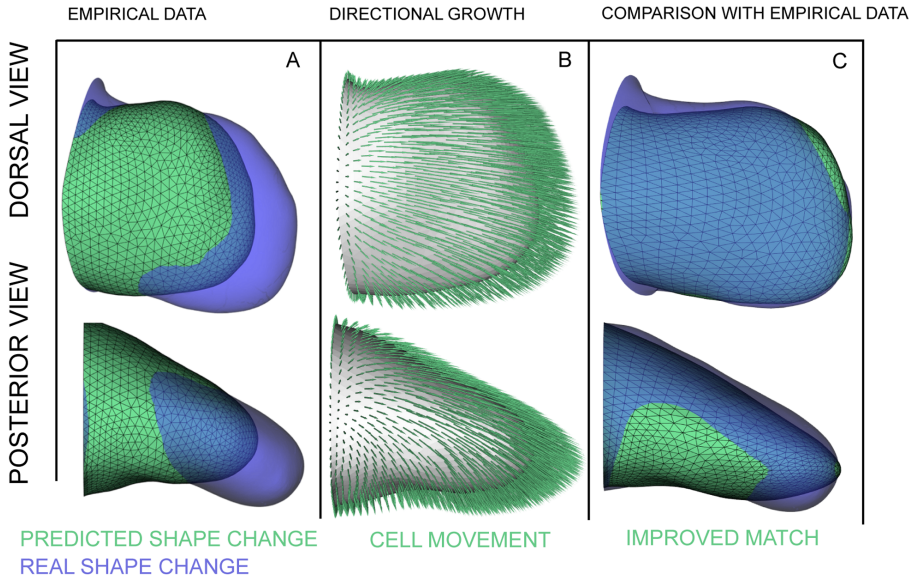

Figure 3.15: **Simulation with directional cell activities.**
Since we have shown that isotropic growth alone is insufficient to explain limb bud shape changes, it is useful to perform a simulation which includes a directional tissue movement, to illustrate how the real growth patterns may appear. In this simulation we combined the measured distribution of isotropic growth (the **s** field, calculated from the Tc data and the measured changes in cell density), with a hypothetical distally-oriented force-field f. The simple addition of this directional force is enough to transform the unsuccessful shape change (A) into a realistic velocity vector field (B) which produces a very accurate predicted shape (C). This reasonable fit to the empirical shape change was achieved just by optimizing the magnitude of the distal force. How the combination of possible directional cell activities (migration, cell intercalation and cell division) combines to create a distally-oriented resultant force, is unclear, but can hopefully be studied in more detail in the future.

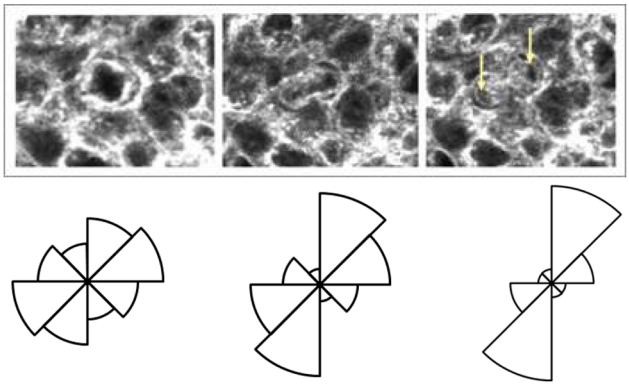

Figure 3.16: **Oriented cell-divisions in mouse limb buds.**
To explore whether the bias in cell division orientation was conserved in the mouse we performed time-lapse imaging of mouse hindlimb buds in culture. Three mouse limb buds were labeled with bodipyceramide, cultured in-vitro and time-lapse imaged with confocal microscopy. This is an alternative measure of cell division orientation, compared to the chick analysis of relative chromatid positions during telophase. (A) Three frames from a time-lapse movie in which a dividing cell can be tracked. (B) The orientation bias of cell divisions from the 3 separate culture experiments. In all 3 cases the bias was seen approximately towards the closest ectoderm, as for the chick.

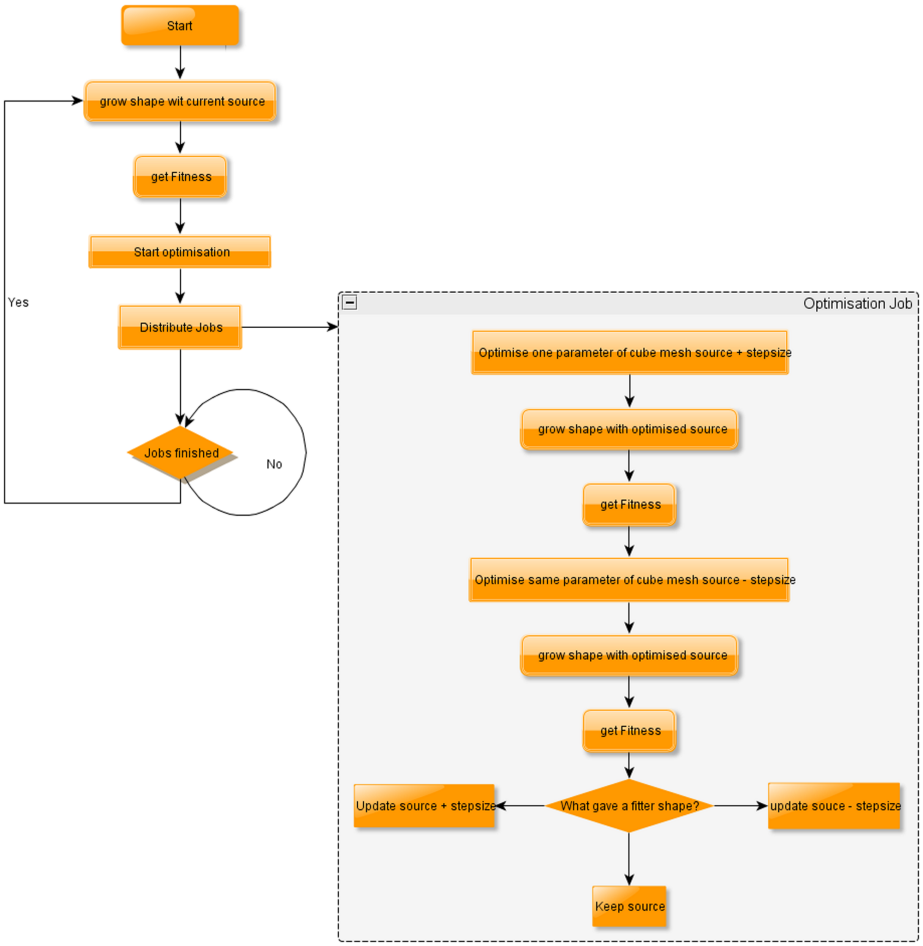

Figure 3.17: **Chart of the parameter optimization process.**
The flow chart demonstrates how the parameter optimization is implemented. A farmer thread splits the problem into smaller jobs that get distributed to a worker thread. When the worker is finished the farmer collects the result and integrates it into the current dataset.

Chapter 4

DISCUSSION

4.1 The cellular mechanisms controlling limb outgrowth

The objective of this thesis was to improve our understanding of the mechanisms driving limb development, especially elongation in the Proximo-distal (PD) axis. To accomplish this, we created a staging system that serves as a formal description of individual developmental steps. This fine-tuned description is critical to put empirical measurements of shape and cell cycle time into a temporal context. The system finds further use as a tool to study highly dynamic underlying genetic processes like Sox9 expression patterning. This tool was employed on two periods during limb development to test a well- accepted hypothesis about the cellular processes driving limb elongation. The general belief has been that limb outgrowth is promoted by a gradient of proliferation rates. A morphogen that diffuses from the distal tip establishes this gradient of high proliferation distally and low proliferation proximally. We demonstrated with a 4D model that the necessary proliferation rates to achieve a realistic elongation are tenfold higher than empirically measured and therefore do not plausibly demonstrate the correct mechanism for outgrowth. Importantly, in this model, cells did not receive any directional informa-

tion of a gradient or the position of the Apical ectodermal ridge (AER), the only constraint was the target shape. Our hypothesis was that other, non isotropic, processes are involved in limb formation. Isotropic cell-proliferation alone can only play a minor role in limb morphogenesis, e.g. to provide enough progenitor cells for ongoing limb development. Based on the results of the simulation presented here, experiments in the lab were designed to investigate these processes and found a strong bias in the orientation of the Golgi apparatus distally and a bias in directed cell division towards the ectoderm. We further discovered complex 3D shapes with highly dynamic filopodia that may be involved in migration or reflect an intercalatory mechanism contributing in tissue movement.
The concept of growth-based morphogenesis is still very popular among limb development biologists and so far, few have argued against it. It is intuitive and supported by the discovery of an actual gradient in cell proliferation and studies of the influence of such a gradient by computer simulation. We validated the existence of this gradient with our own data by quantifying the spatial pattern of cell-cycle times in the mouse limb bud at two developmental stages mE10:15 and mE11:00.
Though this gradient has been reported and further studied, its impact on limb morphogenesis has never been unambiguously scrutinized. In our study [Boehm et al., 2010] we created the first quantitative description of the spatial proliferation pattern which allowed for the systematically testing of the growth-based morphogenesis theory. By quantification, simulation, and parameter optimization we followed the Systems Biology approach of hypothesis testing.

4.2 Quantification of limb development

Carrying out this context-based test for the reproducibility of growth-based morphogenesis required three types of quantitative data and the formulation and the application of a computational model. In particular, we quantified a) *time* i.e. by using the staging system developed in this thesis, we were able to determine the time-difference between a pair of

limb buds b) *shape*, by 3D scanning of real limb buds, we were able to simulate changes in shape using a realistic 3D domain rather than relying on arbitrary limb shape assumptions c) *spatial proliferation pattern* by BrdU and IddU double labelling we could generate a quantitative proliferation map to apply realistic values to our simulation and directly study their implications on the limb morphology.

4.2.1 Quantification of time - staging a limb bud

The aim of this part of the project was to create a program using the morphological changes in a mouse hind limb bud during development to accurately determine the limb bud age and especially, measure age difference between pairs. The shape presents a challenge because it is asymmetrical and lacks distinct landmarks. Further, shape should be considered independently from the orientation or the magnification of an image of the limb. We therefore applied an outline-based method and described the shape geometry by a curved line to describe the outline of the limb bud. To ascertain the limb was smoothly marked by a curved line, we applied a spline interpolation between user-selected points along the shape. The calculation of angular deviations between equidistant points along the spline quantified the shape as a row/column vector of raw coordinates and angular deviations.
We developed a web-application to quantify a training dataset of approximately 650 limb buds. These limb buds at carefully-controlled gestational ages were used to extract the standard-trajectory of limb development spanning a period of 36h from mE10:21 to mE12:09. Though more stages were defined, this 36h window provides reliable staging with a current accuracy of up to +/-2h.
In our approach we staged a new shape by comparing the digitized outline with each of the limb bud outlines from previously generated standard trajectory datasets. For each limb bud, we computed one genuine difference value based on the Euclidean distance between homologous points. This process is computationally cheap and capable of dealing with inaccurately chosen endpoints of the limb shape because of "overhanging"

regions, which do not correspond on both shapes and are excised so they are not subject to the comparison.
A scale-free version of the staging system was also developed to achieve two different goals: a) The user would be spared the use of a calibrated microscope and keeping track of the size of a pixel in images and b) The staging would be based solely on the limb shape rather than limb size. Otherwise, the system would be difficult to use on older images that do not have defined pixelsize information available. Also, different mouse strains are known to have different length gestation times, so size variation between embryos of different strains would not be a problem for this staging system. A direct comparison of the scale-dependent vs. the scale-free version showed a decrease in accuracy and reproducibility in the latter. In Figure 3.3, a decrease of staging accuracy can be seen by comparing the three different approaches (1) size-dependent (2) Size independent, including pixel information for line segmentation and (3) scale-free. Using the staging system, five users staged the same set of limb buds with a standard variation of σ 48min for (1), whereas in the size-dependent analysis (2), the σ increased to 116 min. In the scale -free version (3), the σ increases up to 360min. Further investigation is required to analyze this problem.

4.2.2 Quantification of shape

Previous simulations in 2D used an approximated representation of the limb bud shape. We wanted to improve limb bud shape representation/simulation by using realistic shape geometry in 3D. By using the previously generated morphometric staging system, we were able to select limb buds for our data-driven simulation in two different developmental phases: mE10:15 where the shape is not very distinct and at mE11:00 where the limb shows a posterior bulging. An empirically measured 3D representation of limb bud shapes at each of these phases was generated by OPT scanning, a 3D microscope technique for mesoscopic size specimens. For each of these limb buds (S_{t0}) we selected a partner (S_{t1}) 6h ahead in development (see Figure 2 A-B,F [Boehm et al., 2010])

as a reference limb to allow unbiased comparison of the results of the simulation with real development. We show the general similarity of limb shapes of the same stage with both, our staging system and by a selection of 6 representative aligned shapes (Figure 3.12. Six hours of development is a short enough time-frame to be computationally efficient but long enough to see sufficient shape change used to judge the results of the simulation. The 3D scans of the whole embryo were reconstructed into an iso-surface (see Figure 2 C-E [Boehm et al., 2010]) and cropped to show only the limb bud. The S_{t0} meshes were subsequently processed with NetGen to improve mesh-quality and produce a tetrahedralized mesh (see Figure 2 G [Boehm et al., 2010]).

4.2.3 Quantification of cellular proliferation

Cell cycle times (Tc) were quantified by timed injections of BrdU and IddU into the pregnant mouse, previously performed in our lab. This pulse-chase technique allowed the measurement of the average Tc time of a group of cells by sequentially labelling them with two different markers over a known time interval. Thirty minutes after the last injection, the mice were harvested, fixed, embedded and the limb buds were sectioned into 7μm thick slices. We tracked the spatial arrangement of the slices to be able to map regions of the slices back into the 3D space of the limb geometry. The slices were stained with DAPI targeting nuclei and two different fluorescent secondary antibodies targeting BrdU and IddU. Next, circular regions on the slides were defined and chosen for analysis. According to the ratios between non-labeled, single-labeled and double-labeled cells, the exact cell cycle times for these regions were calculated. The cell cycle times for the 30 measured regions were then mapped onto the 3D domain of the S_{t0} limb bud by selecting matching vertices, maintaining the spatial alignment of the quantified regions. We interpolated this sparse proliferation distribution by a radial basis function populating the whole 3D domain of the limb bud - creating a fine Tc map that qualitatively represents the mechanism underlying growth based morphogenesis.

4.3 Building a dynamic model of growth

We followed the approach described in [Dillon and Othmer, 1999], who modelled the limb as a viscous incompressible fluid whose volume increases corresponding to a distributed source term **s**, representing the patterns of cell division. The physical properties of embryonic tissue were studied by [Phillips et al., 1977], who found evidence of them showing properties of an elastic solid over short periods of time and liquid-like behaviors over longer periods. Similarly to the Dillon&Othmer approach, we used a modified Navier-Stokes equation to describe the stresses and forces generated by isotropic growth in the mesenchymal cells. The model was implemented as a 3D finite element simulation solved over a 3D domain of the S_{t0} limb buds by a commercial software package [CSIRO, 2006]. This way we extended Dillon&Othmers model by a realistic limb shape in 3D allowing for a realistic shape change in all dimensions. The use of an Arbitrary Lagrangian-Eulerian finite element method allowed to deal with a moving boundary and moving vertices. We performed a comprehensive test for the influence of the viscosity of embryonic tissue, an unknown parameter important for the formulation of the Navier-Stokes equations. Our studies covered a range of six orders of viscosity magnitude ranging from a viscosity equal to that of honey to a viscosity lesser than that of water. We showed the influence of viscosity to be non-significant, and therefore negligible in our study (Figure 3.10). The simulation integrated the previously generated quantitative datasets of the staged, tetrahedralized S_{t0} and the spatial proliferation patterns into a 4D simulation of limb development. We showed that the proliferation patterns for both S_{t0} shapes at mE10:15 and mE11:00 fail to promote realistic limb morphogenesis, but rather result in uniform AP, PD and DV growth. This led us to the conclusion that isotropic proliferation has little impact on limb morphogenesis.

4.3.1 Parameter optimization

We tested our hypothesis, that isotropic proliferation has little impact on limb morphogenesis, by asking the reverse question: If the empirical proliferation pattern fails to show normal morphogenesis, is there a hypothetical proliferation pattern that would? To answer this question, we implemented a parameter optimization algorithm to search the parameter space of every possible combination of spatial proliferation pattern.
Due to the high computational expenses of a single simulation (5-8 min) and the extent of necessary simulations, we chose the Hooke&Jeeves direct search method [Hooke and Jeeves, 1961]. At each iteration of optimization, all spatial parameters are tested individually in a single simulation to assess whether a small local increase or decrease in the local growth rate improves the candidate solution. This test was performed by a fitness-function that compared the result of the simulation with the empirically measured S_{t1} shape and weighted the result. Upon completion of each iteration, a new candidate solution was constructed by combining all the individual improvements, thereby implementing a diagonal move in the fitness landscape. The magnitude of the in- /decrements was reduced during the course of the optimization process to allow finer adjustments as the solution improved, similar to the cooling schedule employed in Simulated Annealing.
The computational expense was further reduced by a coarser spatial discretization. From our experiments, we knew that the proliferation pattern varies smoothly across the 3D space. We implemented a regular, orthogonal grid that is superimposed into the same 3D space as the limb mesh (see Figure 5A [Boehm et al., 2010]). Rather than setting individual parameters for the vertices of the limb-mesh, we parameterized the vertices of the cube-mesh and interpolated the values back to the limb mesh after the simulation. Though this is a coarser way of parameterizing the proliferation values, it reduced redundancies and the amount of parameters to be tested by a significant 90%.
By repeatedly starting the parameter optimization at different positions of the fitness landscape (see Figure 3.13, we showed that the algorithm con-

sistently converges to a similar proliferation pattern, a fine strip of high proliferation distally just under the AER (see Figure 3.13) even though the model didn't contain any information about it. One criticism that we may not be able to rule out is the limited number of only six different starting points. To validate the consistency of such a local search algorithm, it is usually tested with hundreds of different, usually random, start conditions. We had to limit ourselves to six different initial start patterns because a full optimization process could take up to two weeks. To achieve a high confidence in our results, we intentionally chose dissimilar starting conditions. The six starting conditions we selected were: (1) A graded proliferation pattern where the area of highest proliferation is distal, the opposite of the hypothesized pattern, (2) A gradient orthogonal to the hypothesized Antero-posterior (AP), (3) A uniform null condition, (4) A random set of proliferation values, (5) A core of high proliferation in the center of the limb and (6) A set of high proliferation at the outer edges of the limb. Despite the highly diverse nature of these start conditions, we showed that the algorithm converges at a homologous proliferation pattern. This finding increased our confidence that the optimization was finding the right proliferation pattern, one that promotes sufficient limb outgrowth to match a empirically measured, real limb shape.

4.4 Summary and Outlook

In summary, in this PhD thesis we have developed several quantitative data sets of different aspects of limb development. By integrating them into a dynamic model, we were able to test a popular hypothesis describing the processes promoting limb morphogenesis, growth-based morphogenesis. We showed that there is a gradient of high proliferation at the distal tip of the limb vs. a decreasing proliferation towards the proximal end. In the computer simulation we created, we showed that this gradient has little impact on the shaping process of the limb.
We employed a parameter optimization algorithm to search for a hypothetical proliferation pattern that, applied to the model, would show the

expected morphogenesis. This pattern was found and the dramatic difference between the required cell cycle times and the empirically measured data leaves only one conclusion, that growth-based morphogenesis plays only a minor role during the 15h of development analyzed in this thesis.

But there is more to be learned from this discovery: It shows the importance of using quantitative measurements to gain biologic relevant knowledge from simulations. The hypothetical proliferation pattern, discovered by reverse engineering, shows striking similarities with the hypothesis behind growth based morphology. The predicted stripe of high proliferation is located just under the AER even though the model had no information about it included. This on its own complies with the recently reported 2D simulations by Morishita and Poplawski as well as Dillon&Othmers model and extends them into 3D.
As we based our computer simulation on real shapes of the limb we can compare the hypothetical values with experimentally measured proliferation data. Hence the discrepancy between the hypothetical and the empirical pattern became evident and gives rise to serious doubts about the hypothesis of growth based morphogenesis.

With these findings the Wheel of Systems Biology (Figure 1.7) reaches a full circle where now a new hypothesis needs to be postulated, new experiments are designed and new simulations are performed. The lab is now at the begin of this process again and initial studies have shown indicators for other possible mechanisms: The highly dynamic, long filopodial processes of mesenchymal cells could be involved in cell migration but could also show a cell intercalatory mechanism producing tissue movement. Time-lapse imaging could not reveal a single preferential direction for filopodial activity, arguing against a simple model of chemotactic migration towards the AER. The striking orientation of the Golgi-Apparatus and the bias in directed cell-divisions towards the ectoderm in chick and mouse (Figure 3.17) will also lead to interesting new ideas.
The morphometric staging tool will find further use in the study of dy-

namic gene expression patterns and further improvement of the size-independent comparison will enrich its applicability, accuracy and user-friendliness. By the definition of a new standard trajectory a new morphometric staging system could be created - for limbs of different species and ages. Imaginable is even the creation of a staging system for different organs with a similar degree of morphological variability like e.g. the heart or the brain.

Chapter 5

CONCLUSIONS

1. A morphometric staging system was developed to quantify the temporal changes of the developing mouse hind limb. As part of this an outline based method was developed to digitize the shape of a limb and a way to compare limb shapes.

2. A Java Applet was developed to provide a cross-platform user-interface for the staging system. This way a user can upload the limb image and start marking the outline directly in a standard browser. The data is stored in a remote MySql database and can be accessed by the user after logging in to review the staging, change parameters and add new images. Further the data source is improved and can be used to improve the staging system. Figure 3.4 shows the set of Classes and Methods that were created for this project - about 8.000 lines of Java Code.

3. A database scheme was developed storing all relevant information associated with staging a limb bud; see (Figure 3.5); JSON was used as a data exchange format between the Java Applet and MySql.

4. A training dataset of approximately 650 images was analyzed to extract the standard trajectory of limb development. Groups of limb bud shapes of carefully controlled gestational ages, 12 hours apart,

were averaged into a standard shape. Intermediate shapes - one for every hour in between the standard shapes were created by a spline interpolation. This way 61 stages were defined, describing limb development between the gestational ages E10:25 to E12:75.

5. Our study of the validity of "growth-based morphogenesis" was based on two pairs of limb buds accurately staged by the staging system. The first pair was staged as mE10:15 and mE10:21, the second was mE11:00 and mE11:06. Both shapes were processed in the lab into a 3D tetrahedral mesh and a surface mesh.

6. A spatial map of proliferation rates was created my analyzing double-labeled sections of precisely staged limb buds of the same stages as our 3D models. The proliferation rates were calculated for circular regions on the slides and mapped onto the 3D space of the limb shape. By interpolation a full 3D map for the 3D model was created. To rule out the influence of cell condensations on morphogenesis, the changes in cell density were quantified (Figure 3.9).

7. A finite element simulation was tailored to integrate the 3D model of the limb bud and the spatial proliferation pattern into a dynamic simulation of growth.

8. A fitness function was developed to quantify shape difference between a pair of three dimensional objects. For this purpose a 3D data-structure was developed and a set of standard geometrical methods. This Java based framework was further used for other projects in the lab.

9. A parameter optimization algorithm was developed to efficiently search the space of proliferation patterns, to find a pattern that would promote limb development the way it is expected. This piece of software consisted of 3500 lines of ANSI-C code and the algorithm was further parallelized with a farmer-worker method. The farmer generated and controlled single optimization steps (worker

jobs) which were managed by the Sun Grid Engine 6.2 on a 200 node cluster, see Figure 3.17.

10. An interpolation was developed to dramatically decrease the number of calculations during the parameter optimization process. A rectangular grid was superimposed onto the 3D space on the limb model. The parameter optimizations were performed on a spatial coarser grid and linearly interpolated back onto the limb domain.

11. As the empirical pattern dramatically differed from the pattern generated by the parameter optimization, we ruled out the hypothesis of "growth-based morphogenesis" and present evidence for directed cell behaviors.

Chapter 6

LIST OF PUBLICATIONS

6.1 Articles

1. **Boehm, B.**; Rautschka, M.; Quintana, L.; Raspopovic, J.; Jan, Ži. & Sharpe, J.; "A landmark-free morphometric staging system for the mouse limb bud", Development, 2011

2. **Boehm, B.**; Westerberg, H.; Lesnicar-Pucko, G.; Raja, S.; Rautschka, M.; Cotterell, J.; Swoger, J. & Sharpe, J. "The role of spatially distributed cell proliferation in limb bud morphogenesis", PloS Biology, 2010

6.2 Poster Communications

3. **Bernd Boehm**, Henrik Westerberg, Sahdia Raja, James Sharpe, "A data-driven 3D computer model to explore the role of spatially-controlled cell proliferation in limb bud morphogenesis." 11^{th} International Conference on Limb Development, Williamsburgh, US, July 13.-16. 2010

4. **Bernd Boehm**, Henrik Westerberg, Sahdia Raja, James Sharpe "The role of spatially controlled cell-proliferation in limb bud morphogenesis" 2^{th} CRG-PhD Symposium, Barcelona, Spain, Nov. 23. 2009

5. **Bernd Boehm** and James Sharpe "A morphometric limb staging system" MBI Workshop on Morphogenesis, Limb Growth, Gastrulation, Somitogenesis, Neural Tube Formation, Columbus, US, November 17-21., 2008

6. **Bernd Boehm** and James Sharpe "A morphometric limb staging system", 10^{th} International Conference on limb Development and Regeneration, San Lorenzo de El Escorial, Spain, August 13.-16.,2008

6.3 Oral communications

7. **Bernd Boehm** & James Sharpe, "Systems Biology to untangle the complexity of life: exploring the *inverse problem*", Mini-Symposium on clonal analysis and growth, Empuries, Spain, May 24-25 2009

8. **Bernd Boehm** & James Sharpe, "The standard trajectory of limb development", Workshop on growth and development, Perugia, Italy, September 6.-12. 2008

List of Figures

Bibliography

[Ashyraliyev et al., 2009] Ashyraliyev, M., Fomekong-Nanfack, Y., Kaandorp, J., and Blom, J. (2009). Systems biology: parameter estimation for biochemical models. *FEBS Journal*, 276(4):886–902.

[Baena-López et al., 2005] Baena-López, L., Baonza, A., and García-Bellido, A. (2005). The orientation of cell divisions determines the shape of drosophila organs. *Current Biology*, 15(18):1640–1644.

[Barrow et al., 2003] Barrow, J., Thomas, K., Boussadia-Zahui, O., Moore, R., Kemler, R., Capecchi, M., and McMahon, A. (2003). Ectodermal wnt3 β-catenin signaling is required for the establishment and maintenance of the apical ectodermal ridge. *Genes & Development*, 17(3):394.

[Bell et al., 1959] Bell, E., Saunders, J. W., J., and Zwilling, E. (1959). Limb development in the absence of ectodermal ridge. *Nature*, 184(Suppl 22):1736–7.

[Benazet et al., 2009] Benazet, J., Bischofberger, M., Tiecke, E., Goncalves, A., Martin, J., Zuniga, A., Naef, F., and Zeller, R. (2009). A self-regulatory system of interlinked signaling feedback loops controls mouse limb patterning. *Science*, 323(5917):1050.

[Boehm et al., 2011] Boehm, B., Rautschka, M., Laura Quintana, Jelena Raspopovic, v. J., and Sharpe, J. (2011). A landmark-free morphometric staging system for the mouse limb bud. *Development*.

[Boehm et al., 2010] Boehm, B., Westerberg, H., Lesnicar-Pucko, G., Raja, S., Rautschka, M., Cotterell, J., Swoger, J., and Sharpe, J. (2010). The role of spatially controlled cell proliferation in limb bud morphogenesis. *PloS Biology*.

[Bonetta, 2002] Bonetta, L. (2002). Systems biology - the new r&d buzzword? *Nature Medicine*, 8(4):315–316.

[Boogerd, 2007] Boogerd, F. (2007). *Systems biology: philosophical foundations*. Elsevier Science Ltd.

[Bookstein, 1997] Bookstein, F. (1997). *Morphometric tools for landmark data: geometry and biology*. Cambridge Univ Pr.

[Bookstein et al., 1982] Bookstein, F., Strauss, R., Humphries, J., Chernoff, B., Elder, R., and Smith, G. (1982). A comment upon the uses of fourier methods in systematics. *Systematic Zoology*, 31(1):85–92.

[Boot et al., 2008] Boot, M. J., Westerberg, C. H., Sanz-Ezquerro, J., Cotterell, J., Schweitzer, R., Torres, M., and Sharpe, J. (2008). In vitro whole-organ imaging: 4d quantification of growing mouse limb buds. *Nat Methods*, 5(7):609–12.

[Boulet et al., 2004] Boulet, A., Moon, A., Arenkiel, B., and Capecchi, M. (2004). The roles of fgf4 and fgf8 in limb bud initiation and outgrowth. *Developmental biology*, 273(2):361–372.

[Butte and Kohane, 2000] Butte, A. and Kohane, I. (2000). Mutual information relevance networks: functional genomic clustering using pairwise entropy measurements. In *Pac Symp Biocomput*, volume 5, pages 418–429. Citeseer.

[Chan and Thorogood, 1999] Chan, C. and Thorogood, P. (1999). Pleiotropic features of syndromic craniosynostoses correlate with differential expression of fibroblast growth factor receptors 1 and 2 during human craniofacial development. *Pediatric research*, 45(1):46.

[Clough, 1960] Clough, R. (1960). The finite element method in plane stress analysis.

[Cohn et al., 1995] Cohn, M., Izpisúa-Belmonte, J., Abud, H., Heath, J., and Tickle, C. (1995). Fibroblast growth factors induce additional limb development from the flank of chick embryos. *Cell*, 80(5):739–746.

[Cooper et al., 2010] Cooper, K., Wu, S., Jenkins, F., and Tabin, C. (2010). Evolution of hindlimb specialization in the northern three-toed jerboa. *Developmental Biology*, 344(1):435.

[CSIRO, 2006] CSIRO (2006). Fastflo.

[Delaunay, 1934] Delaunay, B. (1934). Sur la sphere vide. *Izv. Akad. Nauk SSSR, Otdelenie Matematicheskii i Estestvennyka Nauk*, 7:793–800.

[Dillon and Othmer, 1999] Dillon, R. and Othmer, H. G. (1999). A mathematical model for outgrowth and spatial patterning of the vertebrate limb bud. *J Theor Biol*, 197(3):295–330.

[Dolbeare et al., 1983] Dolbeare, F., Gratzner, H., Pallavicini, M., and Gray, J. (1983). Flow cytometric measurement of total dna content and incorporated bromodeoxyuridine. *Proceedings of the National Academy of Sciences of the United States of America*, 80(18):5573.

[Dudley et al., 2002] Dudley, A., Ros, M., and Tabin, C. (2002). A re-examination of proximodistal patterning during vertebrate limb development. *Nature*, 418(6897):539–544.

[Ede and Law, 1969] Ede, D. A. and Law, J. T. (1969). Computer simulation of vertebrate limb morphogenesis. *Nature*, 221(5177):244–8.

[Fallon et al., 1994] Fallon, J., Lopez, A., Ros, M., Savage, M., Olwin, B., and Simandl, B. (1994). Fgf-2: apical ectodermal ridge growth signal for chick limb development. *Science*, 264(5155):104.

[Fernandez-Teran et al., 2006] Fernandez-Teran, M. A., Hinchliffe, J. R., and Ros, M. A. (2006). Birth and death of cells in limb development: a mapping study. *Dev Dyn*, 235(9):2521–37.

[Ferson et al., 1985] Ferson, S., Rohlf, F., and Koehn, R. (1985). Measuring shape variation of two-dimensional outlines. *Systematic Zoology*, 34(1):59–68.

[Frey and George, 2000] Frey, P. and George, P. (2000). *Mesh generation: application to finite elements*. Hermes Science Europe.

[Gasseling and Saunders Jr, 1961] Gasseling, M. and Saunders Jr, J. (1961). Effects of the apical ectodermal ridge on growth of the versene-stripped chick limb bud. *Developmental biology*, 3:1.

[George, 1971] George, J. (1971). *Computer implementation of the finite element method*. Stanford University.

[Gong et al., 2004] Gong, Y., Mo, C., and Fraser, S. E. (2004). Planar cell polarity signalling controls cell division orientation during zebrafish gastrulation. *Nature*, 430(7000):689–93.

[Gould, 1991] Gould, S. (1991). The disparity of the burgess shale arthropod fauna and the limits of cladistic analysis: why we must strive to quantify morphospace. *Paleobiology*, 17(4):411–423.

[Gros et al., 2010] Gros, J., Hu, J., Vinegoni, C., Feruglio, P., Weissleder, R., and Tabin, C. (2010). Wnt5a/jnk and fgf/mapk pathways regulate the cellular events shaping the vertebrate limb bud. *Current Biology*.

[Gunz et al., 2005] Gunz, P., Mitteroecker, P., and Bookstein, F. (2005). Semilandmarks in three dimensions. *Modern morphometrics in physical anthropology*, pages 73–98.

[Hall, 2008] Hall, D. H., editor (2008). *C. elegans Atlas*. Cold Spring Harbour Laboratory Press, New York.

[Hamburger and Hamilton, 1992] Hamburger, V. and Hamilton, H. L. (1992). A series of normal stages in the development of the chick embryo. 1951. *Dev Dyn*, 195(4):231–72.

[He et al., 2009] He, X., Zhang, J., and Rzhetsky, A. (2009). On the growth of scientific knowledge: Yeast biology as a case study. *PLoS Comput Biol*, 5(3):e1000320.

[Hecksher-Sorensen and Sharpe, 2001] Hecksher-Sorensen, J. and Sharpe, J. (2001). 3d confocal reconstruction of gene expression in mouse. *Mech Dev*, 100(1):59–63.

[Hooke and Jeeves, 1961] Hooke, R. and Jeeves, T. (1961). Direct search solution of numerical and statistical problems. *Journal of the ACM (JACM)*, 8(2):212–229.

[Hornbruch and Wolpert, 1970] Hornbruch, A. and Wolpert, L. (1970). Cell division in the early growth and morphogenesis of the chick limb.

[Jaeger et al., 2004] Jaeger, J., Blagov, M., Kosman, D., Kozlov, K. N., Manu, Myasnikova, E., Surkova, S., Vanario-Alonso, C. E., Samsonova, M., Sharp, D. H., and Reinitz, J. (2004). Dynamical analysis of regulatory interactions in the gap gene system of drosophila melanogaster. *Genetics*, 167(4):1721–37.

[Jose A. Campos-Ortega, 1993] Jose A. Campos-Ortega, Campos-Orteg, V. H., editor (1993). *Atlas of Drosophila Development*. Cold Spring Harbor Laboratory Press.

[Kirkpatrick et al., 1983] Kirkpatrick, S., Gelatt Jr, C., Vecchi, M., and McCoy, A. (1983). Optimization by simulated annealing. *Science*, 220(4598):671–679.

[Kitano, 2002] Kitano, H. (2002). Systems biology: a brief overview. *Science*, 295(5560):1662.

[Kuhl and Giardina, 1982] Kuhl, F. and Giardina, C. (1982). Elliptic fourier features of a closed contour. *Computer graphics and image processing*, 18(3):236–258.

[Le Novère et al., 2006] Le Novère, N., Bornstein, B., Broicher, A., Courtot, M., Donizelli, M., Dharuri, H., Li, L., Sauro, H., Schilstra, M., Shapiro, B., Snoep, J. L., and Hucka, M. (2006). BioModels Database: a free, centralized database of curated, published, quantitative kinetic models of biochemical and cellular systems. *Nucleic Acids Research*, 34(Database issue):D689–D691.

[Lewandoski et al., 2000] Lewandoski, M., Sun, X., and Martin, G. (2000). Fgf8 signalling from the aer is essential for normal limb development. *Nature genetics*, 26(4):460–463.

[Lin and Perloff, 1985] Lin, A. and Perloff, J. (1985). Upper limb malformations associated with congenital heart disease. *The American journal of cardiology*, 55(13):1576–1583.

[Lo, 1985] Lo, S. (1985). A new mesh generation scheme for arbitrary planar domains. *International Journal for Numerical Methods in Engineering*, 21(8):1403–1426.

[Lohmann, 1983] Lohmann, G. (1983). Eigenshape analysis of microfossils: a general morphometric procedure for describing changes in shape. *Mathematical Geology*, 15(6):659–672.

[Margolin et al., 2006] Margolin, A., Nemenman, I., Basso, K., Wiggins, C., Stolovitzky, G., Favera, R., and Califano, A. (2006). Aracne: an algorithm for the reconstruction of gene regulatory networks in a mammalian cellular context. *BMC bioinformatics*, 7(Suppl 1):S7.

[Mariani et al., 2008] Mariani, F., Ahn, C., and Martin, G. (2008). Genetic evidence that fgfs have an instructive role in limb proximal–distal patterning. *Nature*, 453(7193):401–405.

[Martin and Lewis, 1986] Martin, P. and Lewis, J. (1986). Normal development of the skeleton in chick limb buds devoid of dorsal ectoderm. *Developmental biology*, 118(1):233–246.

[Martynoga et al., 2005] Martynoga, B., Morrison, H., Price, D. J., and Mason, J. O. (2005). Foxg1 is required for specification of ventral telencephalon and region-specific regulation of dorsal telencephalic precursor proliferation and apoptosis. *Dev Biol*, 283(1):113–27.

[Mayr, 1982] Mayr, E. (1982). *The growth of biological thought*. Belknap Press Cambridge, MA.

[Moon and Capecchi, 2000] Moon, A. and Capecchi, M. (2000). Fgf8 is required for outgrowth and patterning of the limbs. *Nature genetics*, 26(4):455–459.

[Morishita and Iwasa, 2008] Morishita, Y. and Iwasa, Y. (2008). Growth based morphogenesis of vertebrate limb bud. *Bull Math Biol*, 70(7):1957–78.

[Navier, 1822] Navier, C. (1822). Mémoire sur les lois du mouvement des fluides. *Mém. Acad. Sci. Inst. France*, 6(2):375–394.

[Nieuwkoop et al., 1967] Nieuwkoop, P., Faber, J., and Gurdon, J. (1967). *Normal table of Xenopus laevis (Daudin)*, volume 2. North-Holland Publ. Co. Amsterdam.

[Niswander, 2002] Niswander, L. (2002). Interplay between the molecular signals that control vertebrate limb development. *International Journal of Developmental Biology*, 46(7):877–882.

[Niswander and Martin, 1993a] Niswander, L. and Martin, G. (1993a). Fgf-4 regulates expression of evx-1 in the developing mouse limb. *Development*, 119:287–287.

[Niswander and Martin, 1992] Niswander, L. and Martin, G. R. (1992). Fgf-4 expression during gastrulation, myogenesis, limb and tooth development in the mouse. *Development*, 114(3):755–68.

[Niswander and Martin, 1993b] Niswander, L. and Martin, G. R. (1993b). Fgf-4 regulates expression of evx-1 in the developing mouse limb. *Development*, 119(1):287–94.

[Ohuchi et al., 1997] Ohuchi, H., Nakagawa, T., Yamamoto, A., Araga, A., Ohata, T., Ishimaru, Y., Yoshioka, H., Kuwana, T., Nohno, T., Yamasaki, M., et al. (1997). The mesenchymal factor, fgf10, initiates and maintains the outgrowth of the chick limb bud through interaction with fgf8, an apical ectodermal factor. *Development*, 124(11):2235.

[O'Rahilly, 1983] O'Rahilly, R. (1983). The timing and sequence of events in the development of the human eye and ear during the embryonic period proper. *Anatomy and Embryology*, 168(1):87–99.

[O'Rahilly and Boyden, 1973] O'Rahilly, R. and Boyden, E. (1973). The timing and sequence of events in the development of the human respiratory system during the embryonic period proper. *Anatomy and Embryology*, 141(3):237–250.

[Pask et al., 2002] Pask, A., Harry, J., Graves, J., O'Neill, R., Layfield, S., Shaw, G., and Renfree, M. (2002). Sox9 has both conserved and novel roles in marsupial sexual differentiation. *genesis*, 33(3):131–139.

[Pearson, 1901] Pearson, K. (1901). Liii. on lines and planes of closest fit to systems of points in space. *Philosophical Magazine Series 6*, 2(11):559–572.

[Pepper and Heinrich, 1992] Pepper, D. and Heinrich, J. (1992). *The finite element method: basic concepts and applications*. Hemisphere Pub.

[Peraire et al., 1987] Peraire, J., Vahdati, M., Morgan, K., and Zienkiewicz, O. (1987). Adaptive remeshing for compressible flow computations. *Journal of computational physics*, 72(2):449–466.

[Petrif et al., 1995] Petrif, F., Giles, R., Dauwerse, H., Saris, J., Hennekam, R., Masuno, M., Tommerup, N., van Ommen, G., Goodman, R., Peters, D., et al. (1995). Rubinstein-taybi syndrome caused by mutations in the transcriptional co-activator cbp.

[Phillips et al., 1977] Phillips, H. M., Steinberg, M. S., and Lipton, B. H. (1977). Embryonic tissues as elasticoviscous liquids. ii. direct evidence for cell slippage in centrifuged aggregates. *Dev Biol*, 59(2):124–34.

[Poplawski et al., 2007] Poplawski, N., Swat, M., Scott Gens, J., and Glazier, J. (2007). Adhesion between cells, diffusion of growth factors, and elasticity of the aer produce the paddle shape of the chick limb. *Physica A: Statistical and Theoretical Physics*, 373:521–532.

[Preparata and Shamos, 1985] Preparata, F. and Shamos, M. (1985). *Computational geometry: an introduction*. Springer.

[Prykhozhij and Neumann, 2008] Prykhozhij, S. and Neumann, C. (2008). Distinct roles of shh and fgf signaling in regulating cell proliferation during zebrafish pectoral fin development. *BMC developmental biology*, 8(1):91.

[Rajan, 1994] Rajan, V. (1994). Optimality of the delaunay triangulation in r d. *Discrete and Computational Geometry*, 12(1):189–202.

[Ramalho-Santos et al., 2000] Ramalho-Santos, M., Melton, D., and McMahon, A. (2000). Hedgehog signals regulate multiple aspects of gastrointestinal development. *Development*, 127(12):2763.

[Reinitz and Sharp, 1995] Reinitz, J. and Sharp, D. (1995). Mechanism of eve stripe formation. *Mechanisms of Development*, 49(1-2):133–158.

[Reiter and Solursh, 1982] Reiter, R. and Solursh, M. (1982). Mitogenic property of the apical ectodermal ridge. *Developmental Biology*, 93(1):28–35.

[Reyment and Jöreskog, 1996] Reyment, R. and Jöreskog, K. (1996). *Applied factor analysis in the natural sciences*. Cambridge Univ Pr.

[Riddle et al., 1993] Riddle, R. D., Johnson, R. L., Laufer, E., and Tabin, C. (1993). Sonic hedgehog mediates the polarizing activity of the zpa. *Cell*, 75(7):1401–16.

[Rohlf, 1990] Rohlf, F. (1990). Morphometrics. *Annual Review of Ecology and Systematics*, 21:299–316.

[Ros et al., 1996] Ros, M., Lopez-Martinez, A., Simandl, B., Rodriguez, C., Izpisua Belmonte, J., Dahn, R., and Fallon, J. (1996). The limb field mesoderm determines initial limb bud anteroposterior asymmetry and budding independent of sonic hedgehog or apical ectodermal gene expressions. *Development*, 122(8):2319.

[Rubin and Saunders, 1972] Rubin, L. and Saunders, J. W., J. (1972). Ectodermal-mesodermal interactions in the growth of limb buds in the chick embryo: constancy and temporal limits of the ectodermal induction. *Dev Biol*, 28(1):94–112.

[Ruppert, 1995] Ruppert, J. (1995). A delaunay refinement algorithm for quality 2-dimensional mesh generation. *Journal of algorithms*, 18(3):548–585.

[Sauer et al., 2007] Sauer, U., Heinemann, M., and Zamboni, N. (2007). Getting closer to the whole picture. *Science*, 316(5824):550–551.

[Saunders and Gasseling, 1968] Saunders, J. and Gasseling, M. (1968). Ectodermal-mesenchymal interactions in the origin of limb symmetry. *Epithelial-mesenchymal interactions*, pages 78–97.

[Saunders, 1948] Saunders, J. W., J. (1948). The proximo-distal sequence of origin of the parts of the chick wing and the role of the ectoderm. *J Exp Zool*, 108(3):363–403.

[Saunders, 1972] Saunders, J. W., J. (1972). Developmental control of three-dimensional polarity in the avian limb. *Ann N Y Acad Sci*, 193:29–42.

[Saunders, 2002] Saunders, J. W., J. (2002). Is the progress zone model a victim of progress? *Cell*, 110(5):541–3.

[Schöberl, 1997] Schöberl, J. (1997). Netgen - an advancing front 2d/3d-mesh generator based on abstract rules. *Comput.Visual.Sci*, 1:41–52.

[Sharpe et al., 2002] Sharpe, J., Ahlgren, U., Perry, P., Hill, B., Ross, A., Hecksher-Sorensen, J., Baldock, R., and Davidson, D. (2002). Optical projection tomography as a tool for 3d microscopy and gene expression studies. *Science*, 296(5567):541.

[Sheets et al., 2006] Sheets, H., Covino, K., Panasiewicz, J., and Morris, S. (2006). Comparison of geometric morphometric outline methods in the discrimination of age-related differences in feather shape. *Frontiers in Zoology*, 3(1):15.

[Shephard et al., 1988] Shephard, M., Guerinoni, F., Flaherty, J., Ludwig, R., and Baehmann, P. (1988). Finite octree mesh generation for automated adaptive three-dimensional flow analysis. *Numerical grid generation in computational fluid mechanics'88*, pages 709–718.

[Shephard and Yerry, 1983] Shephard, M. and Yerry, M. (1983). Approaching the automatic generation of finite element meshes. *Computers in Mechanical Engineering*, 1(4):49–56.

[Shostko and Löhner, 1995] Shostko, A. and Löhner, R. (1995). Three-dimensional parallel unstructured grid generation. *International Journal for Numerical Methods in Engineering*, 38(6):905–925.

[Summerbell et al., 1973] Summerbell, D., Lewis, J., and Wolpert, L. (1973). Positional information in chick limb morphogenesis. *Nature*, 244:492–496.

[Summerbell and Wolpert, 1972] Summerbell, D. and Wolpert, L. (1972). Cell density and cell division in the early morphogenesis of the chick wing. *Nature*, 239(88):24–26.

[Sun et al., 2002] Sun, X., Mariani, F., and Martin, G. (2002). Functions of fgf signalling from the apical ectodermal ridge in limb development. *Nature*, 418(6897):501–508.

[Thacker, 1980] Thacker, W. (1980). A brief review of techniques for generating irregular computational grids. *International Journal for Numerical Methods in Engineering*, 15(9):1335–1341.

[Theiler, 1989] Theiler, K. (1989). *The house mouse : atlas of embryonic development*. Springer-Verlag, New York.

[Tickle, 1981] Tickle, C. (1981). The number of polarizing region cells required to specify additional digits in the developing chick wing.

[Tickle, 2005] Tickle, C. (2005). Making digit patterns in the vertebrate limb. *Nature Reviews Molecular Cell Biology*, 7(1):45–53.

[Wanek et al., 1989] Wanek, N., Muneoka, K., Holler-Dinsmore, G., Burton, R., and Bryant, S. V. (1989). A staging system for mouse limb development. *J Exp Zool*, 249(1):41–9.

[Wang et al., 2011] Wang, B., Sinha, T., Jiao, K., Serra, R., and Wang, J. (2011). Disruption of pcp signaling causes limb morphogenesis and skeletal defects and may underlie robinow syndrome and brachydactyly type b. *Human Molecular Genetics*, 20(2):271.

[Wiener, 1948] Wiener, N. (1948). *Cybernetics of Control and Communication in the Animal and the Machine*. The MIT Press and John Wiley.

[Wolpert, 1968] Wolpert, L. (1968). *The French Flag problem: a contribution to the discussion on pattern development and regulation*, volume Vol. 1 of *Towards a Theoretical Biology*. Edinburgh University Press, Edinburgh.

[Wolpert, 1969] Wolpert, L. (1969). Positional information and the spatial pattern of cellular differentiation. *J Theor Biol*, 25(1):1–47.

[Wyngaarden et al., 2010] Wyngaarden, L., Vogeli, K., Ciruna, B., Wells, M., Hadjantonakis, A., and Hopyan, S. (2010). Oriented cell motility and division underlie early limb bud morphogenesis. *Development*, 137(15):2551.

[Xu et al., 2000] Xu, J., Liu, Z., and Ornitz, D. M. (2000). Temporal and spatial gradients of fgf8 and fgf17 regulate proliferation and differentiation of midline cerebellar structures. *Development*, 127(9):1833–43.

[Yus et al., 2009] Yus, E., Maier, T., Michalodimitrakis, K., Van Noort, V., Yamada, T., Chen, W., Wodke, J., Guell, M., Martinez, S., Bourgeois, R., et al. (2009). Impact of genome reduction on bacterial metabolism and its regulation. *Science's STKE*, 326(5957):1263.

[Zelditch, 2004] Zelditch, M. (2004). *Geometric morphometrics for biologists: a primer*. Academic Press.

[Zhan and Roskies, 1972] Zhan, C. and Roskies, R. (1972). Fourier descriptors for plane closed curves. *IEEE Trans. Comput*, 21(3):269–281.

[Zhang et al., 2010] Zhang, Y., Vibranovski, M., Landback, P., Marais, G., and Long, M. (2010). Chromosomal redistribution of male-biased genes in mammalian evolution with two bursts of gene gain on the x chromosome. *PLoS Biol*, 8(10):e1000494.

[Zimmer, 2008] Zimmer, C. (2008). *Microcosm: E. coli and the New Science of Life*. Random House, Inc.

LIST OF ACRONYMS

AER Apical ectodermal ridge

AP Antero-posterior

BrdU Bromodeoxyuridine

CFD Computational Fluid Dynamics

CT X-ray Computed Tomography

CVA Canonical variates analysis

DAPI 4',6-diamidino-2-phenylindole

DFA Discriminant function analysis

DV Dorso-ventral

EFA Elliptical Fourier analysis

FEM Finite element modelling

Fgf Fibroblast growth factor

HSCR Hirschsprung disease

IddU Iododeoxyuridine

Ihh Indian Hedgehog

KEGG Kyoto Encyclopedia of Genes and Genomes

LPM Lateral-plate mesoderm

LPM Lateral plate mesoderm

mE Morphometric embryonic day

MRI Magnet Resonance Imaging

OPT Optical Projection Tomography

PC Principal component

PCA Principal component analysis

PD Proximo-distal

PDE Partial differential equation

pH3 Phosphorylated-histone H3

SBML Systems Biology Markup Language

Shh Sonic Hedgehog

$\mathbf{S}_{t0}$ Limb-shape at timepoint t_0

$\mathbf{S}_{t1}$ Limb-shape at timepoint t_1

Tc Cell cycle time

TS Theiler stage

WMISH Whole mount in-situ hybridization

ZPA Zone of polarizing activity